

1 **Modeling considerations for research on Ocean Alkalinity Enhancement** 2 **(OAE)**

3 Katja Fennel¹, Matthew C. Long², Christopher Algar¹, Brendan Carter³, David Keller⁴, Arnaud
4 Laurent¹, Jann Paul Mattern⁵, Ruth Musgrave¹, Andreas Oschlies⁴, Josiane Ostiguy¹, Jaime B.
5 Palter⁶, Daniel B. Whitt⁷

6
7 ¹Department of Oceanography, Dalhousie University, Halifax, Nova Scotia, Canada

8 ²National Center for Atmospheric Research, University Corporation for Atmospheric Research,
9 Boulder, Colorado, USA

10 ³Pacific Marine Environmental Laboratory, National Oceanic and Atmospheric Association,
11 Seattle, Washington, USA

12 ⁴Marine Biogeochemical Modelling, GEOMAR Helmholtz Centre for Ocean Research Kiel, Kiel,
13 Germany

14 ⁵Ocean Sciences Department, University of California Santa Cruz, Santa Cruz, California, USA

15 ⁶Graduate School of Oceanography, University of Rhode Island, Narragansett, Rhode Island,
16 USA

17 ⁷Earth Science Division, NASA Ames Research Center, Moffett Field, California, USA

18

19 **Abstract**

20 The deliberate increase of ocean alkalinity (referred to as Ocean Alkalinity Enhancement or
21 OAE) has been proposed as a method for removing CO₂ from the atmosphere. Before OAE can
22 be implemented safely, efficiently, and at scale several research questions have to be addressed
23 including: 1) which alkaline feedstocks are best suited and in what doses can they be added
24 safely, 2) how can net carbon uptake be measured and verified, and 3) what are the potential
25 ecosystem impacts. These research questions cannot be addressed by direct observation alone
26 but will require skillful and fit-for-purpose models. This article provides an overview of the
27 most relevant modeling tools, including turbulence-, regional- and global-scale biogeochemical
28 models, and techniques including approaches for model validation, data assimilation, and
29 uncertainty estimation. Typical biogeochemical model assumptions and their limitations are
30 discussed in the context of OAE research, which leads to an identification of further
31 development needs to make models more applicable to OAE research questions. A description
32 of typical steps in model validation is followed by proposed minimum criteria for what
33 constitutes a model that is fit for its intended purpose. After providing an overview of
34 approaches for sound integration of models and observations via data assimilation, the
35 application of Observing System Simulation Experiments (OSSEs) for observing system design
36 is described within the context of OAE research. Criteria for model validation and
37 intercomparison studies are presented. The article concludes with a summary of
38 recommendations and potential pitfalls to be avoided.

39

40 1 Introduction

41 Ocean Alkalinity Enhancement (OAE) refers to the deliberate increase of ocean alkalinity, which
42 can be realized either by removing acidic substances from or adding alkaline substances to
43 seawater. OAE is receiving increasing attention as a method for removing CO₂ from the
44 atmosphere; such methods are referred to as marine Carbon Dioxide Removal (mCDR)
45 technologies (Renforth and Henderson, 2017). Natural analogues to OAE exist (Shubas et al.
46 2023). An increase in the alkalinity of seawater leads to a repartitioning of its dissolved
47 carbonate species with a shift toward bicarbonate and carbonate ions (Zeebe and Wolf-Gladrow
48 2001, Renforth and Henderson 2017), leading to a reduction in the aqueous CO₂ concentration
49 and thus the partial pressure of CO₂ ($p\text{CO}_2$; Schulz et al. 2023). Since exchange of CO₂ between
50 the ocean and atmosphere occurs when the surface ocean $p\text{CO}_2$ is out of equilibrium with that of
51 the atmosphere, a lowering of the ocean's $p\text{CO}_2$ will lead to a net ingassing of atmospheric CO₂
52 (i.e., an increase in CO₂ uptake by the ocean or a decrease in outgassing due to OAE). This
53 would increase the oceanic and decrease the atmospheric inventories of inorganic carbon, in
54 other words, it would result in mCDR. In contrast to other mCDR technologies, OAE does not
55 exacerbate ocean acidification (Ilyina et al. 2013). In fact, an increase in ocean alkalinity
56 counteracts acidification, and while subsequent net uptake of atmospheric CO₂ largely restores
57 pH to its pre-perturbation value, there is potential for OAE deployment to mitigate acidification
58 impacts near injection sites (Mongin et al. 2021).

59 Several important research questions should be addressed before implementing OAE as an
60 mCDR technology at scale. These include: 1) which alkaline substances are best suited and in
61 what doses can they be added reliably while avoiding precipitation of calcium carbonate (which
62 would decrease alkalinity and could result in runaway precipitation events), 2) how can
63 changes in alkalinity and net carbon uptake be measured, verified, and reported (referred to as
64 MRV; see Ho et al. 2023) to enable meaningful carbon crediting, and 3) what are the potential
65 ecosystem impacts and how can harm to ecosystems be avoided or minimized while
66 maximizing potential benefits. These research questions cannot be addressed by direct
67 observation alone but will require an integration of observations and numerical ocean models
68 across a range of scales. Skillful and fit-for-purpose models will be essential for addressing
69 many OAE research questions including the MRV challenge, assessment of environmental
70 impacts, and interpretation of natural analogs.

71 Ocean models are useful for a broad range of purposes, from idealized models for basic
72 hypothesis testing of fundamental principles to realistic models for more applied uses (see
73 primer on ocean biogeochemical models by Fennel et al. 2022). In the context of OAE research,
74 this full range of models is applicable. For example, idealized models of particle-fluid
75 interaction can inform us about dissolution and precipitation kinetics at the scale of particles,
76 realistic local-scale models can inform us about nearfield processes in the turbulent
77 environment around injection sites, and larger-scale regional or global ocean models can be
78 used to support observational design for field experiments, to demonstrate possible verification
79 frameworks, and to address questions about global-scale feedbacks on ocean biogeochemistry.
80 A common objective of all these modeling approaches is to realistically simulate the spatio-

81 temporal evolution of the seawater carbon chemistry, including alkalinity and dissolved CO₂,
82 and attribute that evolution to physical, chemical, and biological processes. Models that are
83 suitable for this purpose will provide spatial and temporal context for properties that can be
84 observed (but at much sparser temporal and spatial coverage than a model can provide) as well
85 as estimates of properties and fluxes that cannot be directly observed but may be inferred
86 because of known mechanistic relationships or patterns of correlation. Applications of realistic
87 models rely on them being skillful and accurate, requiring that they include parameterizations
88 of the relevant processes, and that they are constrained by observations that contain sufficient
89 meaningful information (what is sufficient depends on the application and research question).
90 Methods for constraining models by observations through statistically optimal combination of
91 both are available. Application of such methods is referred to as data assimilation and provides
92 the most accurate estimates of biogeochemical properties and fluxes (see Fennel et al. 2022 for
93 fundamentals and code examples).

94 Model applications for OAE research include the following four general types:

- 95 • Hindcasts are model applications where a defined time period in the past was
96 simulated. They can be unconstrained—in the sense that no observations are fed into the
97 model except for initial, boundary, and forcing conditions—or constrained, where
98 observations inform the model state via data assimilation. The latter are also referred to
99 as optimal hindcasts or reanalyses.
- 100 • Nowcasts/forecasts are similar to constrained hindcasts but with the simulations carried
101 out up to the present (referred to as nowcasts) or into the future (referred to as
102 forecasts). The latter require assumptions about future forcing and boundary conditions,
103 e.g., from other forecasts, climatology, or assuming persistence.
- 104 • Scenarios are unconstrained hindcasts or forecasts where one or more aspects of the
105 model is systematically perturbed to assess the effect of the perturbation, for example, in
106 paired simulations with and without OAE, one would be the realistic case and the other
107 a scenario (also referred to as counterfactual in this case). These can be used to explore
108 even very unlikely situations, which is often required in comprehensive uncertainty and
109 risk assessment.
- 110 • Observing System Simulation Experiments (OSSEs) for observing system design use
111 unconstrained and/or constrained hindcasts to evaluate the benefits of different
112 sampling designs and optimize deployment of observational assets for a defined
113 objective, including tradeoffs between different types of observation platforms.

114 Successful implementation of models to support OAE research and MRV is challenging because
115 of the general sparseness of relevant biogeochemical observations, and the limited lab,
116 mesocosm, and field trial data available to date for model parameterization. Further, models are
117 built at a process level and integrated to reveal behavior at the emergent scale. As such, models
118 comprise a collective hypothesis of the ocean's physical, biogeochemical, and ecosystem
119 function—but it is important to recognize that model formulations of key processes related to

120 OAE remain uncertain. It may well turn out that parameterizations of the carbonate system, of
121 plankton diversity and trophic interactions, small scale turbulence, submesoscale subduction
122 and restratification processes, and air-sea gas exchange in the current generation of models
123 require improvement to robustly treat OAE-related questions.

124 The intended scope of this article is to provide an overview of the most relevant modeling tools
125 for OAE research with high-level background information, illustrative examples, and references
126 to more in-depth methodological descriptions and further examples. We aim to provide simple
127 criteria and guidance for researchers on the current state-of-the-art of biogeochemical modeling
128 relevant to OAE research, keeping in mind short-term research goals in support of pilot
129 deployments of OAE and long-term goals such as credible MRV in an ocean affected by large-
130 scale deployment of OAE and possibly other CDR technologies.

131 **2 Modeling approaches**

132 This section provides a brief review of modeling tools available for OAE research with
133 references to more in-depth methodological descriptions and examples, as well as a discussion
134 of which approaches are most applicable to simulating essential processes in different
135 circumstances. The presentation is structured using two complementary organizing principles,
136 the spatial and temporal scales of the problem in Section 2.1 and the biogeochemical and
137 ecological complexity represented by different modeling approaches in Section 2.2. Section 2
138 concludes with a summary of suggested future model development efforts in Section 2.3.

139

140 **2.1. Modeling approaches across scales**

141 In the nearfield, close to the site of an alkalinity increase, an accurate characterization of the
142 spatio-temporal evolution of alkalized waters requires direct representation or parameterization
143 of fluid and particle physics and seawater carbonate chemistry at scales ranging from
144 micrometers to hundreds of meters, spanning turbulent to submesoscale processes (Section
145 2.1.1). In the farfield, covering scales from 10s of meters to 100s of kilometers, where the effect of
146 an alkalinity increase depends less on the details of how the alkalinity was added, or acidity
147 removed, and is instead dominated by ambient environmental processes, local to regional scale
148 models are useful for simulating the impact of alkalinity increases, for verifying the intended
149 perturbations in air-sea exchange of CO₂ and in carbonate system variables, and potentially for
150 simulating ecosystem impacts (Section 2.1.2). Lastly, investigation of the effects of the global
151 ocean's overturning circulation, impacts on atmospheric CO₂ levels, and of Earth system
152 feedbacks resulting from deployment of OAE and other CDR technology at scale requires
153 global modeling approaches (Section 2.1.3).

154

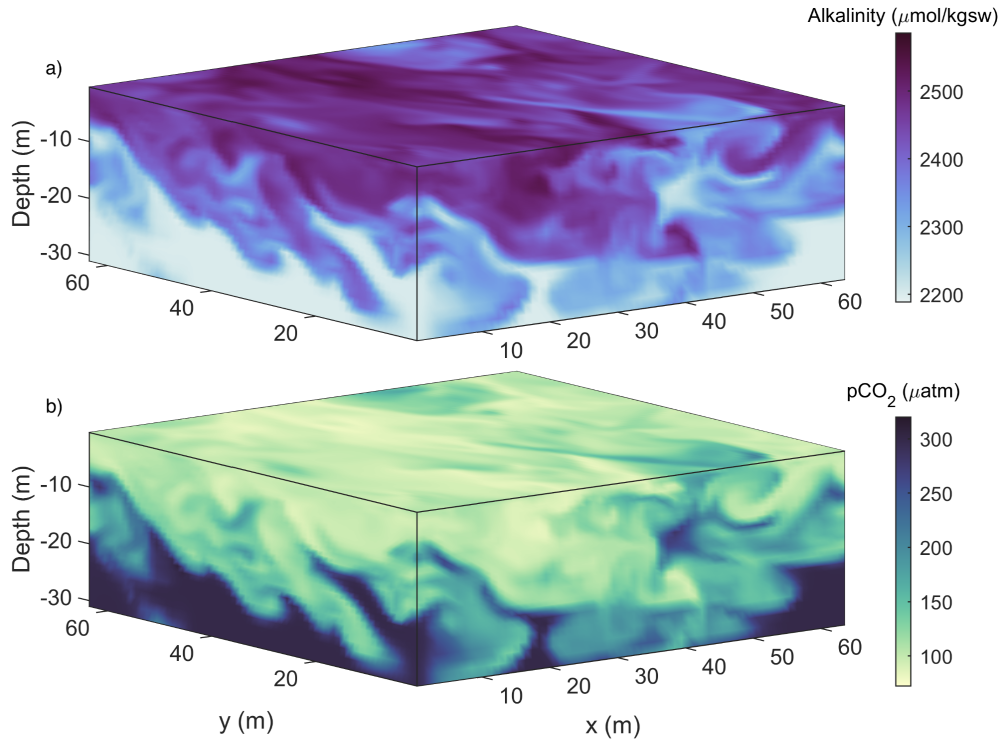
155 **2.1.1. Particle scale to nearfield/turbulence scale (µm to km scales)**

156 Small-scale modeling approaches cover the range from µm-size particles to the turbulent- and
157 submeso-scales in the nearfield of alkalinity additions. Simulating processes on these scales
158 allows one to address questions about how turbulent mixing dilutes and disperses alkalized
159 water and how it affects the settling, aggregation, disaggregation, precipitation, and dissolution

160 of suspended particles. Nearfield modeling has an important role to play in guiding the design
161 of deployment strategies that mitigate environmental impacts and meet future permitting
162 requirements, and to support monitoring. During the initial dispersion and dilution phase of an
163 alkalinity increase in the nearfield, the direct impacts on carbonate system variables are
164 greatest, with waters exhibiting the largest elevations in pH and the highest potential for the
165 formation of secondary precipitates. For particulate alkalinity feedstocks, turbulence close to the
166 deployment site affects dissolution and settling rates, increasing dissolution and either
167 accelerating or diminishing the settling of sedimentary particles compared to the Stokes settling
168 speed (Fornari et al. 2016).

169 Distinct approaches to modeling at these scales involve different levels of parametrization and
170 computational expense, with the relative utility of each approach being dependent on the
171 scientific questions at hand. At the smallest scales, Direct Numerical Simulations (DNS) are the
172 most computationally expensive and specialized class of fluid modeling, as they resolve flows
173 down to the scales at which flow variances dissipate—typically centimeters or smaller in the
174 ocean. Consequently, computational constraints imply that they cannot be run over domains
175 larger than a few meters. DNS are thus integrated over idealized physical domains (i.e., they
176 lack realistic bathymetry) and are suited to investigating fundamental physical processes. For
177 example, multiphase DNS simulations have been used to model the interaction of turbulence
178 with gas bubbles (Farsoiya et al. 2023) and particles (Fornari et al. 2016). Results from such
179 studies provide an important testbed that can be used to develop parameterizations required in
180 lower resolution models.

181 A well-established approach to modeling the fluid flow at scales up to about 10 km uses Large
182 Eddy Simulations (LES), a class of model that directly solves the unsteady Navier-Stokes
183 equations down to the largest turbulent scales on a high-resolution grid. Such models
184 parameterize turbulence using a subgrid-scale model (e.g., Smagorinsky 1963). An advantage of
185 these models is their ability to simulate both an alkalized plume and the environmental
186 turbulence into which the plume emerges. Once alkalized waters enter the surface boundary
187 layer, LES models have an established history of simulating turbulence and mixing that is
188 directly relevant to OAE research (e.g., Mensa et al. 2015, Taylor et al. 2020). An example of an
189 LES simulation of near-surface turbulence dispersing surface-deployed alkalinity downwards is
190 illustrated in Figure 1, where a physical model (Ramadhan et al. 2020) has been coupled to a
191 carbonate solver (Lewis et al. 1998). To date, LES models have rarely been coupled to
192 biogeochemical models due to the computational expenses involved, though their inclusion
193 may be increasingly feasible (Smith et al. 2018, Whitt et al. 2019). As LES simulate flow physics
194 at scales ranging from 10-10,000 m, they do not explicitly resolve the microscales of fluid motion
195 and chemical reactions at particle scales. Nevertheless, the parameterizations of such processes
196 can be included; for example, Liang et al. (2011) used models of bubble concentration and
197 dissolved gas concentration in an LES to examine the influence of bubbles on air-sea gas
198 exchange.



199 **Figure 1:** LES of near surface turbulence coupled to a carbonate system solver. Alkalinity is
 200 added at a rate of $4 \mu\text{mol kgsw}^{-1} \text{m}^{-2} \text{s}^{-1}$ for 20 minutes to the top grid cell at the start of the
 201 simulation. Turbulence, generated by surface wind stress and cooling, sets the rate at which it
 202 mixes downwards (a) along with associated waters of lowered $p\text{CO}_2$ (b). Turbulent plumes and
 203 eddies lead to inhomogeneities in water properties at scales of tens of meters.
 204

205
 206 For alkalinized plumes associated with outfalls from, for example, wastewater treatment plants,
 207 integral models (that assume plume properties such that the governing equations are
 208 simplified) have been developed to examine the initial dilution close to jets and buoyant plumes
 209 up to kilometer scales (Jirka et al. 1996). These models are highly configurable, enabling specific
 210 diffuser configurations as well as the potential to incorporate sediment laden plumes with
 211 particle settling (Bleninger & Jirka 2004). Results are commonly accepted for engineering
 212 purposes, defining mixing zones, and providing a fast “first look” at diffusion and mixing near
 213 an outfall site. However, these models rely on assumptions about the underlying physics of
 214 fluid flow (e.g., axisymmetric plumes and simplified entrainment rates) that may not be
 215 accurate under general oceanic conditions, and results will not include all effects of irregular
 216 bathymetry, finite domain size or arbitrarily non-uniform ambient conditions. Nevertheless,
 217 their simplicity makes them very useful. For example, by combining several simple process
 218 models for plume dilution, particle dissolution, and carbon chemistry, Caserini et al. (2021)
 219 have simulated the initial dilution of slaked lime $\text{Ca}(\text{OH})_2$ particles and alkalinity in a plume
 220 behind a moving vessel.

221 Other methods for modeling at this scale include Reynolds Averaged Navier Stokes (RANS)
 222 and Unsteady RANS (URANS), wherein fluctuations against a slowly varying or time mean

223 background are parametrized, often using constant (large) eddy diffusivities and viscosities.
224 These approaches are often inaccurate at these scales, resulting in simulations that are too
225 diffusive or lacking processes that are of leading order importance to mixing (Golshan et al.
226 2017, Chang & Scotti 2004).

227 There are multiple, potentially interacting sources of uncertainty to consider when evaluating
228 the uncertainty of the applications described above. Perhaps best understood but still
229 problematic is the uncertainty that arises from the computational intractability of simulating all
230 the relevant scales in the μm to km range at once, necessitating the different modeling
231 approaches for different scales, with parameterizations to account for unresolved scales and
232 scale interactions. The dissolved carbonate chemistry of seawater is relatively well
233 parameterized (Zeebe and Wolf-Gladrow 2001), but some modest uncertainties arise from
234 approximations required for computational tractability (Smith et al. 2018). The least understood
235 but potentially dominant source of uncertainty pertains to the representation of the microscale
236 biological, chemical, and physical dynamics of particles, which is an active area of experimental
237 and observational investigation (Subhas et al. 2022, Fuhr et al. 2022, Hartmann et al. 2023).
238 While the explicit multiphase modeling of the particles themselves is computationally costly, an
239 approach wherein the parametrized evolution of inertia-less Lagrangian particles are simulated
240 may provide a fruitful middle ground, providing a mechanism to realistically determine the
241 alkalinity release field associated with the advection, mixing, sinking and dissolution of reactive
242 mineral particles. These questions about particles apply to those released in OAE deployments,
243 as well as particles that precipitate from seawater in part due to OAE deployments, and finally
244 the role of ambient biotic and abiotic particles where OAE is deployed.

245

246 **2.1.2. Local to regional scales (m to km)**

247 Local to regional scale models that range in horizontal resolution from tens of meters to
248 hundreds of kilometers are useful for simulating the impact of alkalinity injections beyond the
249 immediate local area, where conditions do not depend on the details of how the alkalinity was
250 added and instead are determined by regional-scale currents and other process, including the
251 potential for biogenic feedbacks. These models are particularly useful to support OAE field
252 experiments, including planning and observational design, and analysis, integration and
253 synthesis of observations, and to facilitate interpretation of observations from natural analogs.
254 Furthermore, local and regional scale models will likely prove to be indispensable for
255 quantification of OAE effects in research settings, for guiding assessments of its environmental
256 impacts, and for MRV during the potential implementation of OAE. A skillful model can
257 simulate when and where changes in carbonate chemistry and the ensuing anomalies in air-sea
258 CO_2 exchange occur and provide an estimate of the spatio-temporal extent of the
259 biogeochemical properties affected by OAE.

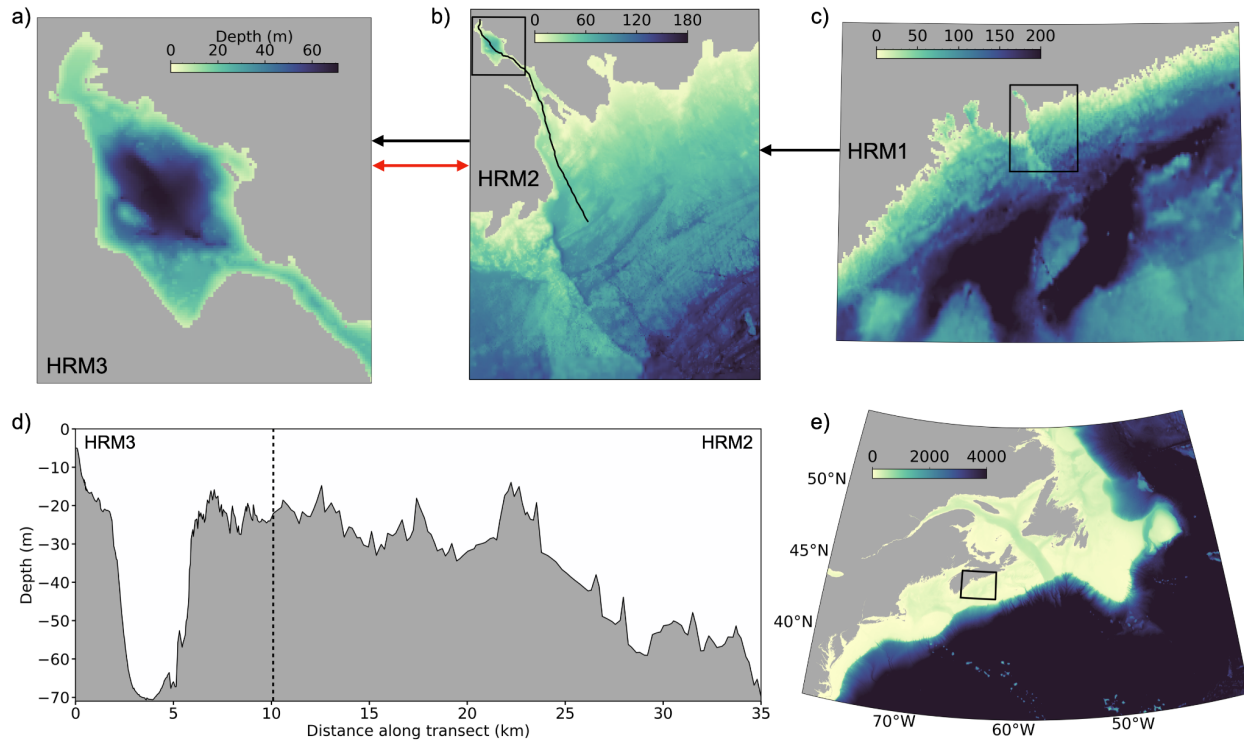
260

261 Regional models have distinct advantages over global models in their ability to resolve the
262 spatial scales on which OAE would be applied both experimentally and operationally, and their
263 documented skill in representing coastal and continental shelf processes more accurately
264 (Mongin et al. 2016, Laurent et al. 2021). Examples of regional model applications in the context

265 of OAE include the recent studies by Mongin et al. (2021) and Wang et al. (2023). Mongin et al.
266 (2021) used a coupled physical-biogeochemical-sediment model tailored to Australia's Great
267 Barrier Reef to investigate to what extent realistic OAE applied along a shipping line could
268 alleviate anthropogenic ocean acidification on the reef. Wang et al. (2023) used a coupled ice-
269 circulation-biogeochemical model of the Bering Sea to study the efficiency of OAE in coastal
270 Alaska.

271
272 Implementation of a regional model in a target domain requires generation of a grid with
273 associated bathymetry, specification of boundary conditions (including atmospheric forcing,
274 information about ocean dynamics along the lateral boundaries of the domain, any fluxes of
275 biogeochemical properties across the air-sea, sediment-water, and land-ocean boundaries, river
276 inputs), and generation of initial conditions within the domain (Fennel et al. 2022). Different
277 circulation models are available for implementation in domains targeted for OAE studies (see,
278 e.g., Table 1 in Fennel et al. 2022), all with distinct strengths and established user communities.
279 Particularly relevant in the context of studying coastal applications of OAE is a model's ability
280 to accurately represent coastal topography, making unstructured grid models and models with
281 terrain-following coordinates particularly attractive. Another feature to be considered is a
282 model's ability to run in two-way nested configurations. In the more widely applied one-way
283 nesting of domains, simulated conditions from a larger scale model (referred to as the parent
284 model) are used to generate the dynamic lateral boundary conditions of a smaller scale, higher
285 resolution model (the child model), which runs off line from the parent model. With two-way
286 nesting, both models run simultaneously and information is exchanged continually along their
287 intersecting boundaries. This allows information generated within the high-resolution child
288 domain (e.g., the spreading distribution of a tracer or alkalinity addition) to be received and
289 propagated by the larger-scale parent model. In this context, model simulations are particularly
290 useful if available in near-real time or in forecast mode. This requires specification of lateral
291 boundary conditions and atmospheric forcing up to the present and into the future. Global
292 1/12th-degree nowcasts and 10-day forecasts of ocean conditions are available from the
293 Copernicus Marine Service (CMEMS 2023) and atmospheric forcing up to the present and 10
294 days into the future are available from the European Centre for Medium Range Weather
295 Forecasts (ECMWF 2023).

296
297 One example of a high-resolution local scale model with two-way nested domains is a
298 framework developed for Bedford Basin in Halifax, Canada (Figure 2, Laurent et al. 2024). The
299 model framework consists of three nested ROMS models (ROMS is the Regional Ocean
300 Modelling System; <https://myroms.org>, Haidvogel et al. 2008, Shchepetkin and McWilliams
301 2005). The outermost ROMS domain has a resolution of 900 m and is nested one-way within the
302 data-assimilative global GLORYS reanalysis of physical and biogeochemical properties
303 (Lellouche et al. 2021). Nested within are two models with increasingly higher resolutions of
304 200 m and 60 m. Depending on the scientific objective to be addressed, the models can be run in
305 one-way and two-way nested mode, where two-way nesting is computationally more
306 demanding, and in hindcast or forecast mode. Implementation of dye-tracers within the model
307 (Wang et al. 2024) allows one to determine dynamic distribution patterns and residence times.



308
309

310 **Figure 2:** Nested configuration of three ROMS models for the Bedford Basin and the adjacent
 311 harbor in Halifax Regional Municipality (HRM). a) The highest resolution model (HRM3; 60 m)
 312 includes the 7 km-long and 3 km-wide Bedford Basin and The Narrows, a 20-m shallow narrow
 313 channel that connects the basin to the outer harbor. b) The larger scale model (HRM2, 200 m)
 314 includes Bedford Basin and Halifax Harbor as well as the adjacent shelf. c) The largest-scale
 315 model (HRM3, 900 m) covers the central part of the Scotian Shelf as indicated in e). d)
 316 bathymetry along a section through HRM3 and HRM2, indicated by the black line in b). Lateral
 317 boundaries of HRM3, HRM2, and HRM1 are shown by black boxes in b), c) and e), respectively.
 318 Black arrows indicate the information flow between models in one way nesting mode. The red
 319 arrow indicates that HRM1 and HRM2 can be run simultaneously with bi-directional flow of
 320 information (two-way coupled mode).

321

322 2.1.3. The global scale

323 A strength of global ocean models is their capacity to comprehensively represent the global
 324 overturning circulation and ocean ventilation. These processes control the time scales over
 325 which waters are sequestered in the ocean interior and determine how long surface waters are
 326 exposed to the atmosphere and can exchange properties, including CO₂, before being injected
 327 back into the ocean interior (Naveira Garabato et al. 2017). Similarly, the large-scale overturning
 328 circulation and the patterns associated with ventilation are important to consider in the context
 329 of deploying OAE at scale, as these patterns exert strong control on the efficiency of OAE at
 330 sequestering CO₂ (e.g., Burt et al. 2021).

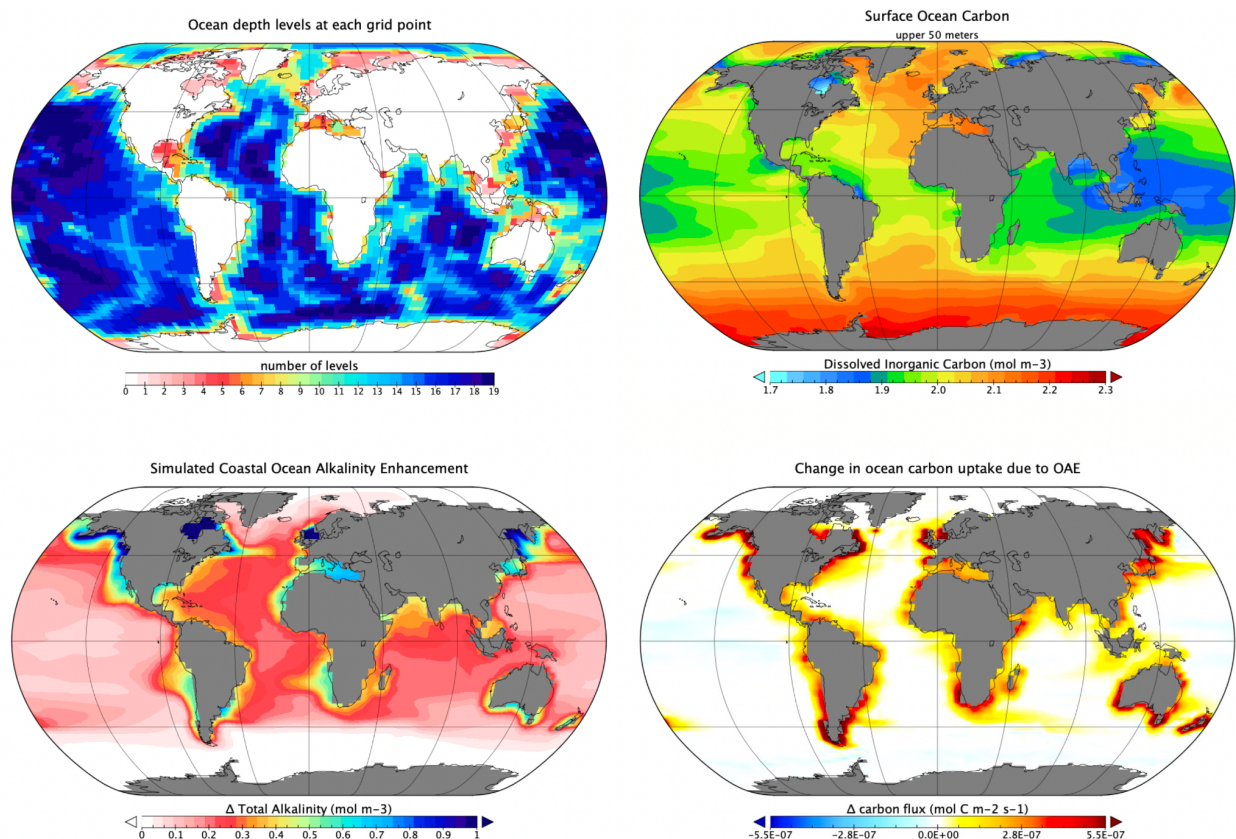
331 When global ocean models are dynamically coupled with models of the land biosphere and the
332 atmosphere, they are referred to as Earth System Models (ESMs) and can be employed to
333 explore Earth system feedbacks to mCDR. In the case of OAE, the main feedback is the change
334 in atmospheric $p\text{CO}_2$ and air-sea gas exchange that will result when CDR approaches are
335 implemented at scale. While regional models have to be forced by atmospheric CO_2
336 concentrations, ESMs represent the atmospheric reservoir and are forced by CO_2 emissions into
337 the atmosphere, which then interacts with land and ocean carbon reservoirs. Only the latter
338 approach can account for OAE-induced reductions in the atmospheric CO_2 inventory which, in
339 turn, would lead to a systematic reduction in air-sea CO_2 fluxes. Regional models and global
340 ocean models that do not explicitly represent the atmospheric CO_2 reservoir and instead are
341 forced by prescribed atmospheric $p\text{CO}_2$ cannot simulate the decline in atmospheric $p\text{CO}_2$ due to
342 OAE. Depending on the alkaline material applied, there may also be feedbacks associated with
343 changes in temperature, albedo, nutrient cycles, and biological responses which can be studied
344 with the help of ESMs.

345 Another important strength of global models relates to the fact that anomalies in air-sea CO_2
346 flux generated by OAE deployments will manifest over large spatio-temporal scales because
347 CO_2 equilibrates with the atmosphere via gas exchange slowly. Alkalinity enhanced waters can
348 be transported far away from injection sites before equilibration is complete (He and Tyka
349 2023). Consequently, OAE signals may exit the finite domain of regional models prior to full
350 equilibration with the atmosphere (e.g., Wang et al. 2023). Because global models represent the
351 entire ocean and can be integrated for centuries and longer, they enable full-scale assessments.

352 A primary challenge for global models, however, is that their horizontal resolution is
353 necessarily limited by computational constraints (see example in Figure 3). Most of the global
354 ocean models contributing the Coupled Model Intercomparison Project version 6 (CMIP6), for
355 example, have horizontal resolutions of about 1° or roughly 100 km (Heuzé 2021) and do not
356 accurately represent biogeochemical processes along ocean margins (Laurent et al. 2021). Model
357 grid-spacing imposes a limit on the dynamical scales that can be explicitly resolved in the
358 models; this is particularly problematic for coarse resolution global models because mesoscale
359 eddies—i.e., motions on scales of about 10–100 km—dominate the variability in ocean flows
360 (Stammer 1997). Since coarse resolution models cannot resolve mesoscale eddies explicitly, the
361 rectified effects of these phenomena, including their role in transporting buoyancy and
362 biogeochemical tracers, must be approximated with parameterizations (e.g., Gent and
363 McWilliams 1990).

364 Notably, the fidelity of the simulated flow in global models, including the imperfect nature of
365 these parameterizations, projects strongly on the model's capacity to accurately simulate
366 ventilation and the associated uptake of transient tracers, such as anthropogenic CO_2 or
367 chlorofluorocarbons (CFCs), from the atmosphere (e.g., Long et al. 2021). Biases in the uptake of
368 transient tracers will also have implications for a model's capacity to faithfully represent the
369 impact of OAE, where the path of alkalinity-enhanced waters parcels in the surface ocean, and
370 their subsequent transport to depth is a key control on the efficiency of carbon removal. Biases
371 in the simulated flow are also an important determinant of the simulated distribution of

372 biogeochemical tracers in the model's mean state. Hinrichs et al. (2023), for example,
 373 demonstrate that inaccuracies in the physical redistribution of alkalinity by the flow is a
 374 dominant mechanism contributing to biases in the alkalinity distributions simulated by CMIP6
 375 models.



376
 377 **Figure 3:** Example of Earth System Model properties and output from the University of Victoria
 378 Earth System Climate Model (Keller et al., 2012, Mengis et al., 2021) including a) the model
 379 bathymetry (depth levels), and b) the simulated present-day dissolved inorganic carbon
 380 concentration (mol m^{-3}) averaged over the upper 50 m of the ocean. Panels c) and d) show
 381 results from a coastal OAE study by Feng et al. (2017) where the change in upper ocean
 382 alkalinity (upper 50 m) and the air-sea flux of CO_2 are shown relative to the RCP8.5 control
 383 simulation. Shown is the Oliv100_Omega3.4 simulation from Feng et al. (2017), where $100 \mu\text{m}$
 384 olivine grains were added to ice-free coastal grid cells in proportion to RCP 8.5 CO_2 emissions
 385 (i.e., 1 mol of alkalinity per mole of emitted CO_2) until a sea surface aragonite Ω threshold of 3.4
 386 was reached.

387 Finally, another important challenge associated with global ocean models is the requirement to
 388 represent the entire global ocean ecosystem with a single set of model parameters (e.g., Long et
 389 al. 2021, Sauerland et al. 2020). In particular, the biological pump is an important control on the
 390 distribution of biogeochemical tracers, including alkalinity and DIC. The magnitude of organic
 391 carbon export, and the magnitude of biogenic calcium carbonate export, are important controls
 392 on the distribution of alkalinity and DIC at the ocean surface and in the interior (e.g., Fry et al.,

393 2015). These quantities are a product of ecosystem function and, since the global ocean is
394 characterized by diverse biogeography (e.g., Barton et al., 2013), capturing global variations in
395 the biological pump presents a challenge.

396 **2.1.4 Integration across scales**

397 Choosing the appropriate modeling tool for a given OAE-related question requires clarity about
398 the scale of the problem to be addressed and the objectives of the model application.

399 Approaches for OAE vary significantly with respect to the spatial footprint of alkalinity
400 increase. Proposed methods for spreading alkalinity feedstocks at the surface ocean include the
401 addition of reactive minerals (e.g., CaO, Ca(OH)₂ or Mg(OH)₂) in ship-propeller washes (e.g.,
402 Köhler et al., 2013, Renforth et al., 2017, Caserini et al., 2021) or using other means (e.g., Gentile
403 et al., 2022) along tracks from commercial or dedicated OAE vessels or through coastal outfalls
404 (e.g., wastewater-treatment or power plants); the addition of less-reactive minerals to corrosive
405 or high-weathering environments (e.g., olivine spreading on beaches or mineral addition to
406 riverine discharge, e.g., Montserrat et al., 2017, Foteinis et al., 2023, Mu et al., 2023); and
407 electrochemically generated point-sources of alkalinity that are discharged as highly alkaline
408 seawater (e.g., House et al., 2009) from existing facilities (e.g., desalination and wastewater-
409 treatment plants), dedicated facilities (e.g., Wang et al., 2023), or from an array of smaller
410 infrastructure (e.g., grids of off-shore wind turbines). Models for OAE research should
411 represent these footprints of alkalinity increases appropriately for the questions being
412 addressed.

413 There are research questions that fall relatively neatly into one of the three scale ranges
414 described above in sections 2.1.1 to 2.1.3. For example, consideration of the nearfield effects of
415 different alkalinity feedstocks (e.g., dissolved versus particles) or analysis of the potential
416 impacts from secondary CaCO₃ precipitation due to elevated alkalinity from a point source
417 require models that resolve the scales of turbulent motion. Examination of the change in air-sea
418 CO₂ flux due to a broad and diffuse alkalinity increase is less demanding on model resolution
419 and regional scale models are appropriate for this question. Investigation of Earth system
420 feedbacks requires ESMs. However, there also are many aspects of OAE that require a bridging
421 of scales. For example, when considering different deployment methods like discharge from
422 vessels into the ocean surface boundary layer versus additions made through outfalls via
423 surface or subsurface plumes, modeling requirements vary. In both cases, the resulting
424 biogeochemical response may be affected by dynamics operating in the nearfield, where
425 conditions are sensitive to the deployment method and turbulence has to be considered, and the
426 far-field, where conditions do not depend on the details of how the alkalinity was added and
427 the air-sea flux of CO₂ is instead determined by ambient environmental processes. Another
428 example is the challenge that anomalies in air-sea CO₂ flux generated by OAE deployments will
429 manifest over large spatio-temporal scales because CO₂ equilibrates with the atmosphere via
430 gas exchange slowly. Some interplay among the modeling tools described in sections 2.1.1 and
431 2.1.2 is likely going to be required. One straightforward approach would be to parameterize
432 small-scale processes in the larger-scale models.

433 2.2 The range of biogeochemical realism & complexity

434 Application of biogeochemical ocean models for the purposes of OAE research and verification
435 requires reevaluation, and likely further development, of several model assumptions and
436 features related to biogeochemical realism and complexity. For example, the internal sources
437 and sinks of alkalinity are typically not explicitly represented in ocean models; this may become
438 necessary in some circumstances but will be challenging (Section 2.2.1). OAE-related
439 perturbations of alkalinity, other carbonate system properties, and addition of macro- and
440 micronutrients contained in some alkalinity feedstocks may result in biological and ecosystem
441 responses that current biogeochemical models are not capable of representing but that would be
442 relevant for the assessment of environmental impacts of OAE and the verification its CDR
443 efficiency (Section 2.2.2). Furthermore, depending on the environmental setting, sediments can
444 be sources or sinks of alkalinity; these sediment-water fluxes need to be appropriately
445 considered, including the potential impacts of OAE on their magnitude, in order to obtain
446 complete and trustworthy carbon budgets (Section 2.2.3). Other boundary fluxes that require
447 accurate specification are alkalinity inputs from rivers and groundwater (Section 2.2.4) and the
448 air-sea flux of CO₂ across the air-sea interface (Section 2.2.5).

450 2.2.1 Representing alkalinity in seawater

451 Alkalinity is an emergent property that depends on the concentrations of numerous chemical
452 species with distinct internal source and sinks (Schulz et al. 2023; Wolf-Gladrow et al. 2007;
453 Middelburg et al. 2020). Skillful simulation of alkalinity in seawater may require explicit
454 representation of its multiple biotic and abiotic sources and sinks, some of which are difficult to
455 constrain. A major process by which alkalinity is consumed is the production of calcium
456 carbonate. In the water column, this is predominantly a biotic process, performed by calcifiers,
457 although “whiting” events, where calcium carbonate precipitates spontaneously from in
458 ambient seawater can be locally important (e.g., Long et al. 2017).

459
460 Models vary in the degree of mechanistic sophistication with which biogenic calcification is
461 represented. For example, some models explicitly resolve calcifiers, such as pelagic
462 coccolithophores (e.g., Krumhardt et al. 2017) and foraminifera (Grigoratou et al. 2022) and, in
463 some cases, also benthic corals, foraminifera, or calcifying higher trophic levels and thus can
464 mechanistically account for the associated alkalinity consumption. Alternatively, models can
465 parameterize biotic production of carbonate, and its subsequent sinking and dissolution, as a
466 fraction of organic matter production combined with an assumed remineralization profile (e.g.,
467 Schmittner et al. 2008; Long et al. 2021). Dissolution of carbonate minerals produces alkalinity,
468 at the sediment surface and in the water column as carbonate particles sink. This can be
469 represented with first-order abiotic dissolution kinetics with a dependence on the saturation
470 state of ambient water in the water column (e.g., Sulpis et al., 2021), in the sediments (e.g.,
471 Emerson & Archer, 1990) or in micro-environments in aggregates or organisms (Barrett et al.,
472 2014) with systematic differences for different crystal structures, aragonite and calcite (Morse et
473 al., 1980).

474

475 Production of alkalinity occurs via uptake of nitrate or nitrite by photoautotrophs, while
476 remineralization consumes alkalinity when happening aerobically but generates alkalinity
477 when occurring anaerobically, e.g. via denitrification (Fennel et al. 2008). Biotic production and
478 consumption of alkalinity is stoichiometrically coupled to the release or uptake of nutrients and
479 carbon, where non-Redfield processes such as nitrogen fixation or denitrification need to be
480 specifically considered in the stoichiometric relationships (Paulmier et al., 2009).

481
482 Spontaneous precipitation of carbonate minerals in pelagic environments could occur when
483 seawater is highly oversaturated with respect to carbonate (Moras et al. 2022) but is, to the best
484 of our knowledge, not yet included in ocean models. When simulating OAE approaches that
485 may generate high oversaturation with respect to carbonate, spontaneous precipitation of
486 carbonates needs to be considered, especially when condensation nuclei are present.
487 Appropriate approaches will have to be developed, e.g., using near-field models to
488 mechanistically represent this process and a meta-model approach to develop
489 parameterizations that are suitable for far-field and larger-scale models.

490
491 Organic compounds produced within the ocean or originating from land can also act as proton
492 acceptors and contribute organic alkalinity (e.g., Koeve and Oschlies 2012, Ko et al. 2016,
493 Middelburg et al. 2020) and will impact the carbonate system, the partial pressure of CO₂ and
494 thus the air-sea CO₂ flux. Commonly, the contribution of organic alkalinity is deemed small
495 enough in oceanic environments to be negligible, but this assumption should be reconsidered in
496 the context of OAE, especially for coastal CDR deployments where the organic contribution to
497 alkalinity is thought to be larger. To the best of our knowledge, models do not account for
498 organic alkalinity. A better quantitative understanding of organic contributions to alkalinity is
499 likely needed to parameterize or mechanistically represent its contribution in models. Similarly,
500 it may be important in the context of mineral OAE deployments to account for local variations
501 in [Ca²⁺] and [Mg²⁺] to accurately estimate the *p*CO₂ anomalies generated by different OAE
502 feedstocks. While these constituents have very long residence times in the ocean, and are hence
503 commonly assumed to vary conservatively in proportion to salinity, variations in their relative
504 abundance has an impact on the thermodynamic equilibrium coefficients used to solve seawater
505 carbonate chemistry (Hain et al., 2015).

506 **2.2.2 Representing biological and ecological processes**

508 A key question related to OAE is whether changes in carbonate chemistry induce differential
509 responses in organisms. In the pelagic zone, OAE might shift the phytoplankton community
510 composition, for example, due to distinct physiological sensitivities of different groups (e.g.,
511 Ferderer et al. 2022). Further, if OAE is accomplished via rock dissolution, carbonate versus
512 silicate rock may impact the relative balance between phytoplankton functional groups (PFTs)
513 such as calcifiers and diatoms, and changes in Mg and Ca ratios may also influence calcification
514 (Bach et al., 2019). Additionally, ancillary constituents specific to particular feedstocks may have
515 biological activity. Silicate rocks include bioreactive metals such as Fe, a micronutrient with the
516 capacity to stimulate phytoplankton growth, and others that are can be toxic when occurring in

517 high concentrations, such as Ni and Cu, and may adversely impact phytoplankton and reduce
518 primary productivity (Bach et al., 2019). The bioreactivity of these metals may be difficult to
519 simulate in models as their dissolved concentrations can be partially mediated by complexation
520 with organic ligands (Guo et al., 2022). Physical impacts of OAE feedstocks may also have
521 important biological impacts through changes in the propagation of light in the surface ocean,
522 and direct exposure to mineral particles may have additional impacts, e.g., on zooplankton
523 through particle ingestion (Harvey, 2008; Fakhraee et al., 2023). Effects of OAE on plankton
524 have the potential to propagate to higher trophic levels through marine food webs as the
525 magnitude and quality of net primary productivity shifts and trophic energy transfer is altered
526 accordingly.

527
528 Simulating this full collection of processes in models is challenging. Dominant modeling
529 paradigms for simulating planktonic ecosystems include PFT- and trait-based models (e.g.,
530 Negrete-Garcia et al., 2022). In these systems, physiological sensitivities are parameterized
531 according to transfer functions that modulate rate processes—growth, for instance—on the basis
532 of ambient environmental conditions. Nutrient limitation of growth is often represented using
533 Michaelis–Menten kinetics wherein growth rates decline as nutrients concentrations become
534 limiting. State-of-the-art ESMs represent PFTs with multiple nutrient co-limitation, which is
535 essential to effectively simulate plankton biogeography of the global ocean. Diatoms, for
536 example, are capable of high growth rates, enabling them to outcompete other phytoplankton
537 under high-nutrient conditions, but their range is restricted to high latitudes and upwelling
538 regions where there is sufficient silicate. If OAE were to modulate the concentration of
539 constituents represented by multiple nutrient co-limitation models, it is possible such models
540 could simulate the phytoplankton community response—though it’s important to consider
541 whether the models provide representations that are sufficiently robust for the magnitude of
542 OAE-related perturbations. In some cases, models are missing key processes that would be
543 required to mechanistically simulate certain effects. We are aware of no models that represent
544 Ni toxicity, for instance. Including these effects, as well as a capacity to simulate secondary
545 interactions, such as ligand complexation of metals in OAE feedstocks, will require significant
546 investment in empirical experimentation to understand essential rate processes and
547 physiological responses.

548
549 Shortcomings in the capacity of models to represent physiological responses to OAE is an
550 important consideration for the ability of models to faithfully represent ecological impacts.
551 Notably, electrochemical OAE techniques present a simpler set of processes to consider than
552 using crushed-rock feedstocks, where ancillary constituents and physical dynamics come into
553 play. For electrochemical OAE, the most likely biological feedback to consider relates to the
554 impacts of changing carbonate chemistry on biogenic rates of calcification or phytoplankton
555 growth rates (Paul and Bach 2020). It is also possible that carbon limitation of phytoplankton
556 growth (Paul and Bach 2020; Riebesell et al. 1993) may also be important. Empirical research
557 exploring physiological sensitivities should be used to develop prioritizations of key model
558 processes comprising early targets for implementation. Model documentations should use
559 consistent stoichiometric relations to link alkalinity changes to those of nutrients and carbon

560 (Paulmier et al. 2009) and state the assumptions made about carbonate formation and
561 dissolution.

562

563 **2.2.3 Representing sediment-water exchanges**

564 The exchange of solutes between the sediments and overlying water influences ocean
565 chemistry, including the properties of the carbonate system (Burdige 2007). Depending on
566 location and time scale, OAE may affect these exchanges and should be appropriately
567 considered in models. Sediments influence the marine carbonate system primarily through the
568 remineralization of organic matter, which returns DIC to overlying water (and alkalinity if this
569 remineralization occurs anaerobically), and the dissolution of biogenic silicate or carbonate
570 minerals. CaCO_3 is of particular importance as its dissolution releases alkalinity, while its burial
571 is an alkalinity sink, and the balance between the two is a key control on the ocean's alkalinity
572 balance over timescales approaching 10^4 years (Middelburg et al. 2020). Furthermore,
573 remineralization and other microbial metabolisms, such as "cable bacteria," can significantly
574 lower pore water pH by several pH units below seawater values (Meysman and Montserrat
575 2017). This can drive dissolution of CaCO_3 and generate alkalinity in the sediments, even in
576 shallow waters when the overlying water is supersaturated (Rau et al. 2012).

577

578 Representing these processes in coastal and shelf sediments (< 200 m) is challenging. Shallow
579 water depths and high productivity result in a significant delivery of organic matter to the
580 sediments that is much larger than in the deep ocean. As a result, the relative importance of
581 sediments in organic matter remineralization is larger and production of alkalinity by anaerobic
582 metabolisms is more important in these shallow sediments than in the deep ocean (Seitzinger et
583 al. 2006, Jahnke 2010, Huettel et al. 2014, Chua et al. 2022). In addition, these environments are
584 dynamic with organic supply and bottom water conditions varying on tidal, seasonal, and
585 interannual timescales. Accounting for the exchange between sediments and overlying water
586 and its variability on tidal, seasonal, and interannual timescales will likely be necessary in
587 regional and global biogeochemical models that aim to simulate alkalinity cycling in coastal and
588 shelf seas, even for relatively short simulation durations of months to years.

589

590 The choice of approach to modeling sediments may depend on the sediment type. For example,
591 the mechanisms transporting solutes across the sediment-water interface can be divided into
592 two categories depending on the sediment's grain size. In coarse sediments, i.e. permeable
593 sands, pressure gradients drive flow through the seabed replenishing sediment oxygen content
594 (Huettel et al. 2014). Organic carbon stores are low and remineralization was long thought to be
595 primarily aerobic. However, evidence has emerged relatively recently that anaerobic
596 remineralization in sandy sediments is more important than originally thought (Chua et al. 2022
597 and references therein). Idealized models that represent the three-dimensional sediment
598 structure illustrate the importance of turbulence and oscillatory flows in permeable sediments
599 (see Box 2 in Chua et al. 2022). These models are highly localized and computationally
600 demanding, prohibiting their coupling with ocean biogeochemical models. Thus, permeable

601 sediments are currently not well represented in regional or global ocean biogeochemical
602 models.

603
604 In cohesive, fine-grained sediments with low permeability, i.e. muds, transport is limited by
605 diffusion or faunal mediated mixing and exchange processes, i.e. bioirrigation or bioturbation
606 (Meysman, et al. 2006, Aller 2001). In these environments, detailed multicomponent reactive-
607 transport models of sediment biogeochemistry – so called diagenetic models – can reproduce
608 carbon remineralization rates partitioned between aerobic and anaerobic pathways,
609 precipitation/dissolution reactions between sediment grains and porewaters, and the transport
610 of solutes across the sediment-water interface (Boudreau 1997, Middelburg et al., 2020). These
611 mechanistic models will be useful for detailed investigations into how perturbations of the
612 carbonate system in seawater overlying the sediments affect their biogeochemistry and for
613 addressing questions about the potential influence of particulate alkalinity feedstocks settling to
614 the seafloor (Montserrat et al. 2017, Meysman and Montserrat 2017). However, typically these
615 models are one-dimensional and applied to a few representative locations. Coupling fully
616 explicit diagenetic models to three-dimensional ocean biogeochemical models, while
617 conceptually straightforward, is computationally prohibitive. Instead, depth-integrated
618 sediment processes have been implemented as bottom boundary conditions (e.g., Moriarty et al.
619 2017, 2018, Laurent et al. 2016). For example, Laurent et al. (2016) used a diagenetic model in a
620 “meta-modeling” approach to estimate bottom boundary nutrient fluxes for a regional scale
621 biogeochemical model. By parameterizing the diagenetic model with detailed geochemical data
622 (porewater profiles and nutrient fluxes) from a few individual locations, then forcing it over a
623 range of expected bottom water conditions, they developed empirical functions relating
624 sediment fluxes to bottom water conditions that could be used to parameterize bottom
625 boundary conditions in the water column model. A similar approach could be used in OAE
626 models to parameterize how sediment biogeochemistry may alter alkalinity fluxes, for example,
627 how redox sensitive processes, such as coupled nitrification-denitrification or sulfate reduction
628 coupled to pyrite burial, both of which may produce alkalinity (Soetaert et al. 2007), may
629 respond to changes in bottom water oxygen or organic matter loading.

630
631 When considering the long-term storage of CO₂ in global-scale ESMs, the interactions between
632 sediments and the deep ocean (> 1000 m bottom depth) may need to be considered. In this
633 environment most organic matter remineralization occurs in the water column, and the small
634 amount of organic matter reaching the seafloor is remineralized aerobically with little to no
635 release of alkalinity. In this case, sediment remineralization can likely be either ignored or
636 implemented as a reflective boundary condition where the simulated POC flux to the seafloor is
637 immediately returned as DIC and remineralized nutrients. However, the dissolution or
638 preservation of CaCO₃ in deep sediments is critical to controlling deep water alkalinity and may
639 be important in model simulations that aim to quantify OAE effects on the timescales associated
640 with the large-scale global overturning circulation. CaCO₃ solubility increases with pressure
641 and decreasing pH and CaCO₃ eventually becomes undersaturated at depth. The depth at
642 which sinking CaCO₃ balances its dissolution is referred to as the carbonate compensation
643 depth (CCD). An increase in bottom water CO₃²⁻ or CaCO₃ deposition, will deepen the CCD,

644 burying CaCO_3 , trapping alkalinity, and lowering the alkalinity budget of the ocean.
645 Conversely if CaCO_3 rain rate or CO_3^{2-} concentration decreases, the CCD will shoal and
646 previously buried CaCO_3 will dissolve releasing alkalinity to the deep ocean. CCD
647 compensation therefore opposes any forcing of the deep ocean carbonate system and therefore
648 dampens the rise of CO_2 in the atmosphere but will also counteract any potential OAE solution
649 (see Renforth and Henderson 2017 for a detailed explanation). Although most CaCO_3
650 dissolution occurs in the sediments, there is no consensus as to the level of detail this needs to
651 be represented in models. Some global models employed to investigate large-scale OAE include
652 calcium carbonate dynamics at the sediment surface (Ilyina et al. 2013) others disregard this
653 process (Keller et al. 2014).

654
655 Often global models will parameterize CaCO_3 burial as a function of saturation state, such an
656 approach is effective for resolving CCD dynamics over geological timescales ($\sim 10,000$ y), but not
657 over the century to millennial timescales of CCD readjustment. Models that fully couple
658 sediment diagenesis can resolve these dynamics (Gehlen et al. 2008), but the computational
659 demand can make them ineffective. One solution is the approach of Boudreau et al. (2010) and
660 (2018). By suggesting that CaCO_3 dissolution dynamics are controlled by transport of
661 dissolution products across the benthic boundary layer, they were able to derive equations
662 predicting CCD depth and CaCO_3 dissolution based on bottom water CO_3^{2-} and CaCO_3 rain rate
663 and avoiding a detailed representation of the sediments. These equations, combined with model
664 bathymetry, can parameterize sediment CO_3^{2-} flux as a boundary condition and suitably account
665 for transient sediment CaCO_3 dissolution in large scale ESMs while avoiding the computational
666 demands of a fully coupled ocean circulation-diagenesis model.

667 *2.2.4 Representing river and groundwater fluxes*

669 Regional and global ocean biogeochemical models typically account for river inputs, including
670 their contributions to alkalinity and DIC. In most models this is done by specifying alkalinity
671 and DIC concentrations in imposed riverine freshwater fluxes, although accurate prescription of
672 these concentrations can be challenging. Typically, a combination of direct river measurements,
673 where available, output from watershed models (e.g., Seitzinger et al. 2010), or extrapolations of
674 coastal ocean measurements to a freshwater endmember (e.g., Rutherford et al. 2021) are used.
675 Solute inputs from groundwater are typically ignored but could be important locally. In high-
676 resolution coastal domains near urban areas, sewage input may be an additional important
677 source of carbon, nutrients, and alkalinity.

678
679 It is important to note that land-based CDR applications may have an important effect on ocean
680 alkalinity dynamics through riverine and groundwater delivery of solutes. Terrestrial OAE
681 equivalents broadly referred to as Enhanced Rock Weathering (ERW) rely on the application of
682 lime or pulverized silicate or carbonate rocks on land and in rivers. These strategies aim to
683 generate CO_2 uptake locally but yield a leaching flux of bicarbonate into freshwater systems and
684 subsequent transport into the coastal ocean. Field trials and some commercial applications are
685 currently underway, most of them with the implicit or explicit assumption that the enhanced

686 delivery of alkalinity will generate a carbon removal in the ocean (Köhler et al., 2010; Taylor et
687 al., 2016; Bach et al., 2019). There is a need for coordinated efforts to improve quantification of
688 background riverine fluxes and establish initiatives to effectively track the solute additions from
689 ERW.

690

691 2.2.5 Representing air-sea gas exchange

692 The calculation of air-sea gas exchange is necessary for the quantification of net carbon uptake
693 from OAE in models. Biogeochemical models typically represent this exchange using a bulk
694 relationship that depends on the product of the gas transfer velocity and the effective air-sea
695 concentration difference (Fairall et al. 2000). However, the gas transfer velocity remains highly
696 uncertain and is sensitive to a collection of processes that vary across scales, including sea state,
697 boundary layer turbulence, bubble dynamics, and concentrations of surfactants. The most
698 widely used parameterizations of the gas transfer velocity use empirical fits to observations to
699 construct a functional relation dependent on wind speed only, under the premise that
700 turbulence and bubbles (via the breaking of surface gravity waves) are predominantly
701 determined by wind stress (Wanninkhof 2014). This neglects processes that could be regionally
702 important such as convection, modification by biological surfactants, rain and wave-current
703 interactions, while vastly simplifying the effects of wave breaking and bubbles. Although
704 different dependencies on wind speed have been proposed (quadratic, cubic, hybrid),
705 parameterizing the gas transfer coefficient as a quadratic function of the 10-meter wind speed is
706 the most common (Wanninkhof 1992; Wanninkhof 2014). This relationship is supported by
707 direct measurements of air-sea flux at intermediate wind speeds (3-15 m/s), but at low wind
708 speeds (< 3 m/s), non-wind effects can have an important impact on gas transfer. At high wind
709 speeds (> 15 m/s), breaking waves and bubble injection enhance gas exchange for lower
710 solubility gasses such as CO₂ (Bell et al. 2017). Therefore, quadratic fits tend to underestimate
711 the gas exchange at low and high wind speeds (Bell et al. 2017).

712

713 More complex air-sea exchange parameterizations account for processes such as bubbles, near
714 surface gradients and buoyancy driven convection (e.g., Liang et al. 2013, Fairall et al. 2000), but
715 they depend upon a wider range of input variables. Other considerations in estimating flux
716 arise from the nonlinear dependence on these variables, e.g., wind speed, which can lead to
717 underestimates when made using daily averages rather than hourly measurements (Bates and
718 Merlivat 2001).

719

720 Notably, the gas transfer velocity (k_w) determines the kinetics of gas exchange, given a
721 perturbation in surface ocean $p\text{CO}_2$ away from equilibrium. The timescale for CO₂ equilibration
722 over the surface mixed layer can be fully quantified using the following expression,

$$723 \tau_{gas-ex} = \left(\frac{\partial \text{CO}_2}{\partial \text{DIC}} \right)^{-1} \left(\frac{h}{k_w} \right)$$

724 where h is the depth of the surface mixed layer and the partial derivative $\partial \text{CO}_2 / \partial \text{DIC}$ captures
725 the thermodynamic state of the carbon system chemistry in seawater, specifically with respect
726 to the amount that dissolved CO₂ changes per unit change in DIC (Sarmiento and Gruber 2006).

727 This property is related to the buffer capacity and varies in roughly linear proportion to the

728 carbonate ion concentration. The magnitude of $\left(\frac{\partial \text{CO}_2}{\partial \text{DIC}}\right)^{-1}$ is typically about 20, which explains
729 why the equilibration timescale for CO₂ is so long. The contribution of uncertainty in the gas
730 exchange velocity to overall uncertainty in carbon uptake from OAE deployments will depend
731 in part on the circulation regime involved. For example, in situations where alkalinity-enhanced
732 water parcels are retained at the surface for timescales that are significantly longer than $\tau_{\text{gas-ex}}$,
733 full equilibration will occur and the impact of uncertainty in the gas exchange velocity will have
734 limited influence on the overall uncertainty.

735
736 Even though OAE-induced additional air-sea CO₂ fluxes will, even in hypothetical massive
737 deployments, amount to at most a few Gt CO₂/yr, which is typically not more than a percent of
738 the atmospheric CO₂ inventory, this subtle difference in the treatment of the atmospheric
739 boundary condition can be significant. Using prescribed atmospheric $p\text{CO}_2$ that is unresponsive
740 to marine CDR-induced air-sea CO₂ fluxes has been shown to overestimate oceanic CO₂ uptake
741 by 2%, 25%, 100% and more than 500% on annual, decadal, centennial, and millennial
742 timescales, respectively (Oschlies 2009). Simulations with prescribed atmospheric $p\text{CO}_2$ need to
743 take such systematic biases into account.

744 **2.3 Model development needs for OAE research**

746 While there is already substantial capacity for simulating ocean biogeochemical dynamics at
747 global to regional scales, the discussion above implicates several areas where additional efforts
748 are required to fully establish a modeling capability suitable for supporting OAE. These fall into
749 four primary areas: (1) supporting multi-scale simulations with sufficiently high-fidelity flow
750 fields; (2) faithfully simulating the near-field dynamics associated with alkalinity addition; (3)
751 capturing feedbacks to OAE owing to biological and geochemical responses; and (4) identifying
752 whether there are reduced-complexity modeling approaches that might provide sufficiently
753 robust estimates of the net effects of OAE.

754 As elucidated above, a primary consideration related to capturing OAE impacts is the fidelity of
755 the simulated flow. Notably, OAE presents a somewhat novel use case requiring an effective
756 multi-scale modeling capability. A conceptually straightforward path to improving the
757 representation of ocean circulation and mixing is to increase the resolution of the model grid.
758 However, the computational demand of high-resolution simulations can only be met over more
759 limited-area domains. Since the spatiotemporal footprint of OAE-related perturbations is likely
760 to be large, there will be a need to represent large regions. An argument might be made,
761 however, that the circulation in proximity of an OAE site is most important to capture with
762 high-fidelity. This can be achieved with two-way nested regional models as described in see
763 Section 2.1.2 but will require further development to couple in the nearfield models described in
764 Section 2.1.1. Native grid-refinement, e.g. via unstructured grids, is another approach that may
765 be pursued to effectively support OAE research.

766 The second area of model development relates to the requirement of faithfully representing the
767 dynamics associated with alkalinity addition. Regional to global scales are the most relevant for
768 simulating the air-to-sea exchange of CO₂ ensuing from OAE. It is important, however, to

769 ensure that local processes affecting the mass fluxes and initial dispersal of alkalinity are
770 handled appropriately. As illustrated above, DNS or LES simulations (section 2.1.1) can be
771 leveraged to develop parameterizations for larger-scale models, including for crushed-rock
772 feedstocks where particle dynamics may be important or techniques involving alkalinity
773 enhanced streams entering the ocean from outfall pipes. In addition to process fidelity, there are
774 also numerical constraints to consider. For example, advection schemes used in most ocean
775 general circulation models struggle to represent sharp gradients; large mass fluxes of alkalinity
776 into single model grid-points are likely to cause advection errors that may contaminate aspects
777 of the model solutions making interpretation difficult. More specifically, conservative advection
778 schemes can be characterized in terms of their accuracy, monotonicity (i.e., ability to preserve
779 sign), and linearity (i.e., ability to preserve additivity) and there are always tradeoffs to make
780 between these properties. Research may be required to determine which schemes are best
781 suited to the particular challenges associated with representing the advection of OAE signals.

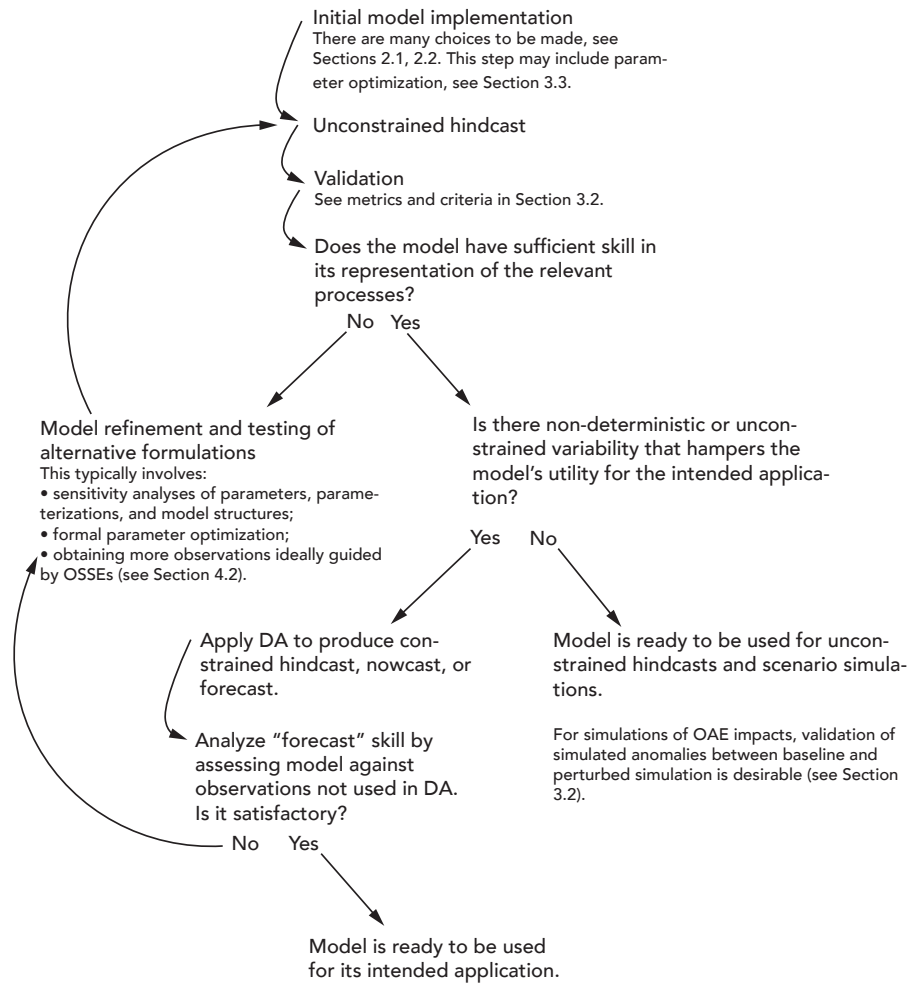
782 The third area of model development relates to our capacity to fully capture the range of
783 biogeochemical feedback associated with OAE. The class of processes to consider here is
784 potentially large and many have been touched on in section 2.2.1 to 2.2.3. Precipitation
785 dynamics, specific elemental components of alkalinity, biogenic responses mediated by
786 physiological or ecological sensitivities, impacts and processes controlling the cycling of
787 ancillary constituents, and accurate sediment-water exchange are all areas that merit
788 consideration. Further efforts are required to understand and prioritize these areas of potential
789 development and, notably, their relative importance is likely to be regionally dependent.

790 Finally, it is important that models be tailored to address specific questions of relevance. In this
791 context, it may be important to consider how much model complexity is required to capture the
792 effects of perturbations, seeking parsimonious representations that are well-supported by
793 empirical constraints and invoking wherever possible a separation of concerns to isolate the
794 factors contributing to uncertainty. For example, there are several near-field considerations that
795 might be addressed using a combination of local observations and ultra-high-resolution
796 modeling tools to generate estimates of alkalinity mass fluxes that are subsequently imposed as
797 forcing in regional- to global-scale models. Another key question is how important it is to
798 comprehensively simulate the mean state to faithfully capture the response to OAE
799 perturbations for the purpose of MRV. For example, if it can be documented that biological
800 feedbacks to OAE are of negligible concern, the core target for simulating OAE effects for MRV
801 may be to capture the cumulative integral of air-sea CO₂ exchange associated with the induced
802 surface ocean *p*CO₂ anomaly. The mean state of the seawater carbon system is relevant here as
803 the background DIC and alkalinity fields determine the *p*CO₂ response per unit addition of
804 alkalinity, but fully prognostic calculations of nutrient cycling may not be necessary.

805 **3 Model validation and integration with observations**

806 Whether a model is useful for OAE research depends on how accurately it represents the
807 physical, chemical, and biological processes that are relevant to the specific research question to
808 be addressed. Model validation, the evaluation of a model's performance, and estimation of

809 uncertainties in model output should thus be integral parts of model implementation and
 810 application. It is important to note that any model, even after best efforts have been made to
 811 improve formulations and conduct the most thorough validation, will deviate from reality. Any
 812 model is, by definition, a simplification of the real world and thus its output will be subject to
 813 uncertainties. Deviations of the model state from the real world can be reduced by applying
 814 statistical techniques, collectively referred to as Data Assimilation (DA) methods, that combine
 815 models with observations and yield the best possible estimates. The steps typically involved in
 816 model implementation and validation, and possible integration with observations through data
 817 assimilation are shown in Figure 3. In this section, we summarize the most important
 818 observation needs for model validation (Section 3.1), briefly describe typical metrics for model
 819 validation and articulate a reasonable minimum criterion (Section 3.2), give a high-level
 820 explanation of approaches for the formal statistical combination of models with observations
 821 through parameter optimization and state estimation (Section 3.3), and describe approaches for
 822 the specification of uncertainty in model outputs (Section 3.4).
 823



824
825

826 **Figure 3:** Typical steps in model implementation and validation.

827 3.1 Observation types for validation

828 Two fundamental requirements for models to be useful in the context of OAE research are high-
829 fidelity representations of physical transport due to advection and mixing, and of
830 biogeochemical effects of OAE, most importantly changes in the inorganic carbon properties.

831 Observations for validation of the simulated physical transport of alkalized waters include
832 temperature and salinity distributions, direct measurements of currents, surface drifter
833 trajectories, sea surface height observations from satellite altimetry, and estimates of
834 geostrophic flow derived from the latter. Additional metrics relevant for assessing the fidelity of
835 the large-scale overturning circulation in global models include combinations of biogeochemical
836 concentration and transient tracers. For example, oxygen can be useful for identifying large-
837 scale transport pathways, even though it convolutes dynamical and biological information.
838 Particularly valuable for assessing large-scale ocean transport on the timescales relevant for
839 OAE are abiotic transient tracers such as such as chlorofluorocarbons (CFCs), sulfur
840 hexafluoride (SF₆), and possibly the isotopes ³⁹Ar and ¹⁴C. Observational approaches for
841 validation at regional scales include explicit tracer studies for documenting dispersion
842 properties using Rhodamine dye or SF₆.

843 In addition to the dynamics of the flow, model validation for OAE research requires the
844 assessment of the fidelity of simulated carbonate chemistry variables (e.g., alkalinity, total
845 dissolved inorganic carbon or DIC, pH, *p*CO₂) and salinity and temperature, which are used to
846 calculate the 13 thermodynamic equilibrium constants and conservative chemical species
847 needed to constrain seawater acid-base chemistry in oxygenated seawater. Depending on the
848 OAE approach and the model application, assessment may also require observed macronutrient
849 (e.g., nitrate, silicate, or phosphate), micronutrient (e.g., Fe), and contaminant (e.g., Ni, and Cr)
850 measurements; bulk seawater properties related to biogeochemical cycling (e.g., dissolved
851 organic carbon content [DOC], particulate inorganic carbon [PIC], chlorophyll fluorescence);
852 and biogeochemical rates and fluxes (e.g., net community calcification).

853 It is not always feasible to obtain the ideal carbonate system observations for model validation.
854 Temperature and salinity can be measured reliably across all ocean depths and, with greater
855 uncertainty and only at the ocean surface, remotely from satellites. The technical capacity for
856 seawater pH measurements is evolving rapidly and sensors and systems now exist for pH
857 measurements across nearly all depths, though the depth-capable systems require regular
858 recalibration (e.g., Maurer et al., 2021). Similarly, there are numerous ways to observe surface
859 ocean *p*CO₂ using a variety of crewed, autonomous, and fixed-location platforms (e.g., ship-
860 based, Saildrone, and moored systems). However, interior-ocean *p*CO₂ observations remain
861 challenging to obtain due to the need for calibration gasses and a gas-water interface. Alkalinity
862 titrations are predominantly performed on discrete bottle samples collected by hand, though
863 autonomous titration systems are under development that enable *in situ* surface time series
864 measurements (Shangguan et al., 2022). Microfluidic *in situ* alkalinity titrators are also under
865 development that consume less reagent per sample but currently show higher uncertainties
866 than discrete samples (Sonnichsen et al. 2023). Solid state titrators that generate acid titrant *in*

867 *situ* show promise for surface and subsurface alkalinity titrations, but these sensors are still
868 undergoing development and validation (Briggs et al., 2017). DIC observations combine the
869 limitations of current measurement systems for both the $p\text{CO}_2$ and alkalinity, and there are only
870 a handful of automated DIC titration systems rated for surface ocean measurements (e.g.,
871 Fassbender et al. 2015; Wang et al. 2015; Ringham 2022). Theoretically, measurement of two of
872 the carbonate system parameters in combination with temperature and salinity and some
873 additional assumptions allows calculation of the other carbonate system parameters in
874 seawater. Unfortunately, the pair of $p\text{CO}_2$ and pH, which are the most accessible to autonomous
875 measurement among the carbonate system parameters, provide nearly identical information
876 about the system. Thus, the results of the calculations that use this pair have higher
877 uncertainties than other combinations (Dickson and Riley 1979; Millero 2007; Cullison Gray et
878 al. 2011; McLaughlin et al. 2015; Raimondi et al. 2019) and are therefore not ideal as a pair for
879 model validation.

880 **3.2 Validation metrics and approach**

881 Validation relies on comparing the model output to observations, often in an iterative loop
882 where the evaluation of a hindcast simulation is followed by model refinements followed in
883 turn by a new hindcast and re-evaluation (Figure 3, Rothstein et al. 2006). Several evaluation
884 metrics are commonly used (see Box 3 in Fennel et al. 2022). The three most common are the
885 root-mean-square error (RMSE), the bias, and the correlation coefficient. All three are relative
886 measures without any objective criterion that indicates which range of values is acceptable or
887 unacceptable. In contrast, the Z-scores, which consider variability within the observational data
888 set, and the so-called model efficiency or model skill, which quantifies whether the model
889 outperforms an observational climatology are two metrics with built-in criteria as to whether a
890 model's performance is acceptable or not (Fennel et al. 2022). Since no single metric provides a
891 complete picture of a model's skill, multiple complementary metrics should always be used in
892 combination (Stow et al. 2009). Furthermore, different points in space and time, and a breadth of
893 variable types should be part of any comprehensive validation because a model may provide
894 accurate estimates for some variables, locations, or times but perform poorly for others (Doney
895 et al. 2009).

896 For OAE research, validation can be considered as a two-step challenge. First, it is necessary to
897 validate unperturbed model baselines to gain confidence that the natural variability is
898 represented appropriately and to quantify model uncertainties. One should compare model-
899 simulated spatial fields and time-series at strategic locations with appropriate observations to
900 assess the model's skill at representing mean distributions as well as the variability for
901 carbonate chemistry measurements and other relevant properties using several of the
902 complementary quantitative metrics listed above. A model could be considered as sufficiently
903 validated when mean distributions, their seasonal variability, and the timing and magnitude of
904 events (e.g., blooms, physical disturbances) are accurately represented. As described in Section
905 3.1, insufficient availability of observational constraints on carbonate system parameters
906 presents a major challenge in this regard. In models applied for OAE research, it is particularly
907 important to assess whether they realistically capture the distributions and variability of

908 seawater properties that govern sensitivity of the seawater carbonate system; recent work by
909 Hinrichs et al. (2023) shows that the current representation of alkalinity in state-of-the-art
910 models requires improvements.

911 The second, even more difficult step is to test whether a model accurately represents alkalinity
912 additions. OAE-related modeling studies thus far have relied on models that are validated only
913 for baseline conditions. These are useful as sensitivity studies. However, validation of a model's
914 ability to accurately represent the perturbations of an alkalinity addition is ultimately needed to
915 address OAE science questions around environmental impacts and MRV. It is likely that the
916 metrics described above for baseline validation are not suitable for this task. Validation should
917 focus on quantifying whether the model accurately captures the anomalies created by OAE.
918 This requires consideration of the spatial footprint and temporal evolution of perturbations and
919 ideally a close integration of experimental, observational, and modeling efforts. For example, a
920 model that is deemed skillful after baseline validation can be used to estimate the appropriate
921 dosage of alkalinity additions, thus ensuring a measurable signal, and guide the observational
922 strategy; subsequent validation may indicate model shortcomings that were not obvious in the
923 baseline validation (e.g., diverging dissipation rates between model and field observations) and
924 prompt model refinement in an iterative loop of model validation, improvement, and renewed
925 experimental assessment (Figure 3).

926 It is important to note that even with repeated steps of validation and model improvement,
927 there is going to be a limit to the degree of realism that can be achieved with any model. Any
928 model simulation will be prone to errors and uncertainties. Sources of error include inaccuracies
929 in model inputs, numerical approximation schemes, insufficient process understanding, and
930 inaccurate model parameters and parameterizations.

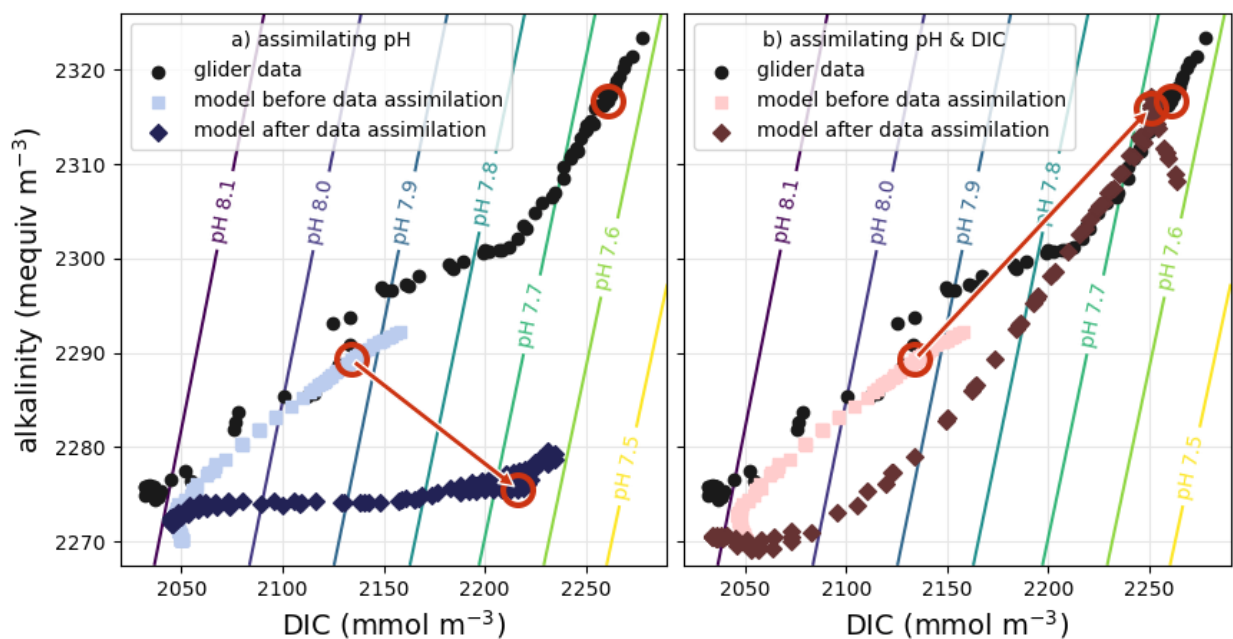
931 **3.3 Data Assimilation**

932 Data assimilation (DA) is the process of improving the dynamical behavior of models by
933 statistically combining them with observations. There are a variety of DA techniques that rely
934 on different mathematical and statistical approaches (Carrassi et al. 2018). Originally developed
935 for numerical weather prediction, DA has been successfully applied to ocean models, including
936 biogeochemical models (Mattern et al. 2017, Cossarini et al. 2019, Ciavatta et al. 2018, Verdy and
937 Mazloff 2017, Teruzzi et al. 2018, Fennel et al. 2019) but success critically depends on the
938 information content of the available observations (Yu et al. 2018; Wang et al. 2020). While DA
939 has been shown to yield large improvements in important parameters governing
940 biogeochemical processes (Mattern et al. 2012, Schartau et al. 2017, Wang et al. 2020) and in
941 model estimates of the physical and biogeochemical model state (Hu et al. 2012, Mattern et al.
942 2017, Ciavatta et al. 2018), it is only starting to be applied to carbonate system properties (Verdy
943 and Mazloff 2017, Carroll et al. 2020, Turner et al. 2023, Figure 4).

944 Application of DA for ocean models is typically applied for one of two purposes: (1) to
945 systematically optimize model parameters, e.g., phytoplankton growth and nutrient uptake or
946 rates of background dispersion, and (2) to estimate the ocean state, e.g., distributions of
947 temperature, phytoplankton biomass, alkalinity (see Fennel et al. 2022 for more details on the

948 practical approaches and examples). The first purpose addresses systematic errors and biases in
 949 models and is useful when systematically modifying and testing different model formulations
 950 while the second assumes an unbiased model and addresses unresolved stochasticity, e.g.,
 951 correcting the locations of mesoscale eddies and current meanders. State estimation offers the
 952 potential to constrain variability such that OAE-induced perturbations of carbonate system
 953 parameters can be documented even if they are smaller than the natural variability in the study
 954 region. Joint estimation of physical and biogeochemical properties is common and can yield
 955 significant improvements for both types of properties (Yu et al. 2018). Hybrid approaches
 956 combining parameter and state estimation have also been proposed (Kitagawa 1998, Mattern et
 957 al. 2012, 2014) but are less widely used.

958



959 **Figure 4:** Example of a DA application for state estimation of carbonate system properties
 960 within a 3-dimensional model of the California Current System. The symbols show glider data
 961 and model estimates at the measurement times and locations; one specific data point and its
 962 associated model estimates are highlighted by red circles. Each data point consists of measured
 963 pH alongside estimated alkalinity and DIC values (see Takeshita et al. (2021) for data source
 964 and details). In the model, pH is a diagnostic variable and primarily dependent on the model's
 965 alkalinity and DIC estimates. (a) When only pH data is assimilated, the model estimates are
 966 moved closer to the observed pH values by increments in alkalinity-DIC space that degrade the
 967 model's alkalinity estimates. (b) The model state estimates improve considerably by
 968 assimilating data for DIC (or alkalinity; not shown) together with the pH observations.
 969

970 Successful application of DA critically requires sufficient observations either of the properties
 971 that the model parameters to be estimated depend on or of the state variables that are being
 972 estimated. The most commonly used observation type in biogeochemical DA applications is
 973 satellite-based ocean color observations (Mattern et al. 2017, Ciavatta et al. 2018, Teruzzi et al.

974 2018) which are available at a relatively high temporal resolution and covering large areas of the
975 surface ocean. While these observations are useful for informing model estimates of properties
976 directly linked to processes involving phytoplankton, they provide little information on the
977 carbonate system. Dynamical models are able to quantitatively constrain processes that cannot
978 be measured directly, by inferring them from observable properties, but only if the observations
979 contain enough relevant information about the processes of interest. Hence, one of the biggest
980 challenges facing the application of DA to models of the marine carbonate system, is the
981 sparsity of observations of the marine carbonate system. Observations of pH, pCO₂, alkalinity,
982 and DIC used to be limited to moorings and research cruises but have more recently been
983 extended by automated observing systems, such as gliders, BGC-Argo floats and uncrewed
984 surface vehicles (Bushinski et al. 2019). Although these measurements are becoming more
985 common (Chai et al. 2020), they are still sparse compared to what is typically required for DA
986 applications. In this context, an additional challenge is the problem of underdetermination, i.e.
987 if multiple processes or properties of interest can cause a similar change in an observable
988 property, then observing this property alone may not hold enough information to constrain
989 these processes or properties and more observations are needed (see Fig. 4 and code examples
990 in Fennel et al. 2022). As new platforms are added to the observing system, DA techniques can
991 help guide their optimal deployment and tailor observational programs to the specific needs of
992 OAE applications (see Section 4.3 below). Furthermore, statistical and machine-learning
993 approaches are being developed (e.g., Lohrenz et al. 2018, Bittig et al. 2018, in prep.) that may
994 help overcome the undersampling of carbonate system properties and could feed directly into
995 DA applications.

996 There is an important subtlety to the application of data-assimilative models when quantifying
997 net CO₂ uptake due to OAE, which is highly relevant for MRV. When the net CO₂ uptake is
998 quantified by calculating the difference between two simulations, one with and one without
999 OAE (one of these is realistic, the other counterfactual), it is not appropriate to assimilate
1000 biogeochemical observations of properties affected by the alkalinity enhancement. The
1001 assimilation of alkalinity-related observations to constrain one of the simulations in the pair
1002 would eliminate the ability to make comparisons between the two. However, assimilation of
1003 observations that are unaffected by OAE (e.g., temperature, salinity, oxygen, etc.) can be
1004 applied to both simulations of the pair. Further research and method development are required
1005 to identify the best approaches for leverage DA in this context.

1006 1007 **3.4 Uncertainty analysis**

1008 Model results should be paired with sound qualitative and quantitative uncertainty estimates,
1009 especially when used for practical decisions. Estimating the uncertainty of model simulations,
1010 however, is inherently difficult because typically one is most interested in simulation outputs
1011 for which observations are not available (e.g., unobserved or insufficiently observed properties
1012 or fluxes in the past, properties and fluxes in the future); hence, standard procedures and
1013 metrics for model validation (Section 3.2) are not helpful for this aspect. Uncertainty estimates
1014 could be based on extensive model parameter and configuration sensitivity studies and
1015 comparisons with models that include more realistic representations of uncertain or

1016 parameterized processes. Furthermore, since specification of uncertainty is an integral part of
1017 DA, DA methodologies provide a useful framework for estimating uncertainty, especially
1018 ensemble-based methods.

1019
1020 Any DA application requires uncertainty specification of the observations that are assimilated
1021 and can provide uncertainty estimates of the results of the assimilation procedure. Specification
1022 of uncertainty in the input data is necessary to inform the DA machinery about how much
1023 weight and reach each data point or data type should have in influencing the outcome. The
1024 more realistic the uncertainties of the input data, the better the DA outcomes in terms of
1025 explanatory or predictive skill. It is important to note that “better” does not mean more precise
1026 in this context. Overconfidence in the accuracy of assimilated observations will lead to
1027 overfitting and a degradation of predictive skill. In the case of parameter optimization, the
1028 output of the assimilation exercise is a set of optimized parameters. The uncertainty of optimal
1029 parameters, referred to as *a posteriori* errors, is determined by a Hessian analysis of the cost
1030 function in combination with the uncertainty of the input parameters before optimization, the
1031 so-called *a priori* errors (Thacker et al. 1989, Fennel et al. 2001). In the case of ensemble-based
1032 state estimation, the ensemble spread of the reanalyzed model state provides a spatially and
1033 temporally resolved estimate of the uncertainty of the reanalysis (Yu et al. 2018, Hu et al. 2012).

1034
1035 However, an important caveat is that subjectivity enters the uncertainty specification in all of
1036 these approaches. For example, in the case of parameter optimization the assumed *a priori*
1037 errors, their probability distributions, and the choice of the cost function are subjective and
1038 influence the *a posteriori* errors (but interestingly the values of the observations themselves do
1039 not). In the case of ensemble-based state estimation, the sources of uncertainty inherent in the
1040 model simulation have to be specified and simulated by generating variations within a model
1041 ensemble. Sources of uncertainty include errors in atmospheric forcing and boundary
1042 conditions, model parameters, and structural uncertainty. Uncertainty in forcing and boundary
1043 conditions is often represented by perturbing the time of sampling, uncertainty in parameters is
1044 represented by sampling from a probability distribution (based on *a priori* assumptions about
1045 the uncertainty of each parameter), and the structural uncertainty is typically represented via
1046 brute-force inflation factors that amplify ensemble spread. Yu et al. (2019), Li et al. (2016), and
1047 Thacker et al. (2012) provide examples where different sources of model uncertainty are
1048 accounted for. While the mechanics by which the model ensemble is generated and spreads
1049 over time is thus subjective, grossly inappropriate choices will lead to obviously wrong or
1050 degraded reanalyses. The success of a DA exercise, which is best judged by an evaluation of
1051 whether the predictive power of the model has improved, thus provides a useful reality check
1052 on whether the choices for specifying uncertainty were appropriate.

1053
1054 How can the framework for specifying and estimating uncertainty from model ensembles be
1055 applied in the context of OAE research? Two different cases should be considered here: 1)
1056 model applications where the absolute value of quantities matters for the research question to
1057 be addressed and thus the uncertainty of the simulated output, and 2) applications where
1058 information about the difference between a simulation with and without OAE is of interest and

1059 the uncertainty of this difference (e.g., the net CO₂ uptake and its uncertainty in the context of
1060 MRV). Examples of the first case include studies of the stability of added alkalinity (i.e.,
1061 simulation of runaway calcium carbonate precipitation) and studies about the exposure of
1062 planktonic and benthic communities to high pH. In this case, the ensemble framework
1063 described above can be applied with the caveat that the specification of all the relevant sources
1064 of uncertainty is by no means trivial and subjective to some degree.

1065
1066 The second case is highly relevant for MRV of OAE where one is interested in accurately
1067 quantifying the increase in seawater DIC due to OAE with well characterized uncertainty. In
1068 this case, one would use two simulations that are based on an identical model set-up with only
1069 one difference, namely a source of alkalinity is applied to one (i.e., one of these two simulations
1070 is counterfactual or hypothetical, the other would typically be as realistic as possible). It may be
1071 tempting, and is conceptually straightforward, to apply the ensemble framework for each
1072 model of the pair and combine the resulting uncertainties via error propagation. However, in
1073 practice this would not provide meaningful estimates because there are sources of uncertainty
1074 that are unaffected by OAE (e.g., atmospheric forcing) and accounting for them may
1075 significantly overestimate uncertainty in the estimated net CO₂ uptake. A more appropriate
1076 approach would be to construct an ensemble of model pairs that explicitly accounts for
1077 uncertainty related to the impacts of alkalinity addition. How to specify and simulate the
1078 sources of uncertainty directly resulting from OAE in practice remains an open research
1079 question.

1080 1081 **4 Model experimentation**

1082 In this section, we lay out general objectives for model experimentation in the context of OAE
1083 research and provide a short historical view of how these model studies have evolved (Section
1084 4.1) followed by specific recommendations for Observing System Simulation Experiments
1085 (Section 4.2) and model intercomparisons (Section 4.3).

1086 1087 **4.1 General objectives of model experimentation**

1088 General objectives of OAE modeling include (1) gaining a better understanding of the
1089 biogeochemistry of OAE, including its effectiveness and side effects, (2) supporting
1090 experiments, field trials, or commercial deployments including through the optimization of
1091 observing systems, (3) assessing global carbon-cycle and climate feedbacks, (4) understanding
1092 the role that OAE can play in climate mitigation efforts, and (5) supporting monitoring,
1093 reporting, and verification activities. At a conceptual level, model approaches for OAE can be
1094 classified as belonging into one of two groups: idealized or realistic. Idealized modeling
1095 approaches are typically driven by research questions of a fundamental nature and aim to
1096 develop or test hypotheses or provide improved process understanding while strongly
1097 simplifying a range of potentially complicating factors. They are useful for illustrating cause-
1098 and-effect relationships and the range of plausible outcomes given strong assumptions. In
1099 contrast, realistic modeling approaches aim to include a broad range of contributing factors as
1100 accurately as possible and provide detailed hindcasts or predictions that, if the model has skill,

1101 can be used for a range of practical applications. In practice, the dividing line between idealized
1102 and realistic models is blurry. Of course, no model will ever simulate all aspects of reality,
1103 hence even realistic simulations make many assumptions and are prone to errors from multiple
1104 sources. It can be effective to apply idealized and realistic approaches in a complementary
1105 manner and iteratively.

1106 It is illustrative to review briefly how modeling for OAE research has developed over the course
1107 of the last decade. Much of the early work on OAE used idealized models. Model simulations
1108 were designed to investigate whether the theoretical concept of OAE could remove large
1109 amounts of CO₂ on the global scale. Rather than trying to account for the technical and socio-
1110 economic constraints of OAE deployment, the model experiments were designed to investigate
1111 what would happen if surface alkalinity was homogeneously increased by massive amounts via
1112 a constant addition rate over extremely large regions of the ocean, e.g., in all sea-ice free waters
1113 (Paquay and Zeebe, 2013; Keller et al., 2014; Ilyina et al., 2013; Köhler et al., 2010; Köhler et al.,
1114 2013). These simulated OAE deployments will never be realized, but the model results
1115 suggested that OAE can be viable as a CDR approach. A particular advantage of this idealized
1116 approach is that the effect of OAE was easy to detect against internal model variability, i.e., the
1117 signal to noise ratio is high. The next steps in modeling OAE have remained idealized but have
1118 begun to introduce more constraints and better mechanistic or empirically derived components
1119 as experimental OAE data becomes available. Recently, modeling studies tailored to specific
1120 regions and modes of application have been conducted to support field trials or commercial
1121 deployment (Mongin et al. 2021, Wang et al. 2023). These applications must be as realistic as
1122 possible. None of the modeling studies published to date have simulated an actual OAE field
1123 trial.

1124 **4.2 Recommendations for Observing System Simulation Experiments (OSSEs)**

1125 Observing system simulation experiments (OSSEs) use data-assimilative simulations to design
1126 new, or modify existing, observing systems such that deployments of observing assets, e.g.,
1127 floats, gliders, moorings, or surface vehicles, is optimized. General overviews and best practices
1128 for OSSEs are provided by Halliwell et al. (2015) and Hoffman and Atlas (2016). Examples of
1129 applications to biogeochemical models include Ford (2021), Wang et al. (2020), and Denvil-
1130 Sommer et al. (2021). Their goal is to maximize the information gained from a new or modified
1131 observing system, while keeping the number of required instruments, sensors, or deployments
1132 – and thereby cost and effort – low. OSSEs are especially valuable tools in the context of OAE
1133 research because the marine carbonate system is still undersampled, observing systems need to
1134 be designed and expanded, and new instruments deployed and configured (Boyd et al. 2023).

1135 In practice, this is done with the help of a pair of two different models or model versions, also
1136 referred to as twin experiments, as follows. A simulation of one of the models is considered to
1137 be the “truth.” This simulation is also referred to as the “nature run” and synthetic observations
1138 are generated by subsampling this nature run. This subsampling can be repeated with different
1139 sampling schemes (e.g., different variable types, different numbers of profiles, transects, and/or
1140 fixed location time series, etc.) to represent different configurations of the observing system.

1141 Finally, the synthetic observations are assimilated into the other model for which a non-
1142 assimilative simulation, the so-called “free run,” is also available. The skill of this data-
1143 assimilative simulation, also referred to as the “forecast run,” can be assessed against the free
1144 run using independent observations that are also sampled from the nature run. In this way the
1145 impact of different sets of observations on the data-assimilative model can be measured and
1146 assessed.

1147 While conceptually straightforward, care and consideration are required when setting up
1148 OSSEs. For example, the choice of the two model versions making up the twin is important. If
1149 the models chosen for the truth and forecast runs are versions of the same model
1150 implementation that were generated by perturbing initial, forcing or boundary conditions in
1151 one of them, the method is referred to as the “identical twin” approach. If two different model
1152 types are used, they are “non-identical twins.” The intermediate approach where the same
1153 model type is used but in different configurations (e.g., different physical parameterizations
1154 and/or spatial resolution) is referred to as fraternal twin. The identical twin approach has been
1155 more common in oceanic DA applications although atmospheric OSSEs have shown that it can
1156 provide biased impact assessments (Hoffman and Atlas, 2016) typically because the error
1157 growth rate between the truth and forecast runs is insufficient. A direct comparison of the non-
1158 identical and identical twin approach for an ocean circulation model of the Gulf of Mexico has
1159 been conducted by Yu et al. (2019). In their assessment of the impacts of the existing observing
1160 system (consisting of satellites and Argo floats), the identical twin approach provided overly
1161 optimistic improvements in model skill after assimilation of data from some observing assets
1162 (specifically sea-surface height and temperature) but undervalued the contribution from
1163 temperature and salinity profiles. They concluded that skill assessments and OSSEs using the
1164 non-identical twin approach are more robust. Similar concerns likely apply to OSSEs for
1165 biogeochemical properties, but this remains to be studied systematically.

1166 **4.3 Recommendations for intercomparisons**

1167 A common approach to assessing model uncertainty are coordinated, multi-model studies,
1168 commonly called model intercomparison projects or MIPs. They can be used to explore the
1169 simulated range of model behaviors, to isolate the strengths and weaknesses of different models
1170 in a controlled setting, and to interpret, through idealized experiments, inter-model differences
1171 (IPCC 2013). Carefully designed experiments can also offer a way to distinguish between errors
1172 particular to an individual model and those that might be more universal and should become
1173 priority targets for model improvement (IPCC 2013). These studies rely on common agreed-
1174 upon protocols for simulating certain processes and writing of diagnostic output to ensure that
1175 best practices are followed, and results are comparable (e.g., Griffies et al., 2016). The best-
1176 known model intercomparison project is probably the Coupled Model Intercomparison Project
1177 (CMIP, Eyring et al., 2016), which is currently finishing up its 6th phase. Within CMIP6, the
1178 carbon dioxide removal intercomparison project (CDRMIP; Keller et al., 2018) is the first project
1179 to develop a model intercomparison experiment for ocean alkalinity enhancement. This and
1180 other MIP examples, including those conducted at smaller region scales (Wilcox et al., 2022),
1181 provide a blueprint for developing coordinated multi-model experiments.

1182 The following key practices have proven useful in previous coordinated multi-model
1183 comparisons. Since broad participation is typically desired, the protocol should be
1184 straightforward for modeling groups to implement, otherwise few will have the resources to
1185 participate. In practice this means avoiding new implementations of complex code or requiring
1186 too many or too long simulations. If applicable, forcing data should be centrally prepared and
1187 provided to participants in a standardized way that enables easy modification or reformatting,
1188 if needed, for use with different models. Using common simulations that modeling groups are
1189 likely to have completed already, e.g., climate change scenarios, as control runs and
1190 experimental branching points is helpful for minimizing the number of additional required
1191 simulations. It is useful to establish common practices that facilitate the production and analysis
1192 of the model output, e.g., what should be archived and shared (Jukes et al., 2020) and data
1193 standards governing the structure and required metadata for model output (Pascoe et al., 2020).
1194 Shared software to standardize model output, such as the Climate Model Output Rewriter
1195 (CMOR; <https://cmor.llnl.gov/>) commonly used in CMIP, can be helpful. To maximize the use of
1196 model output, it should be made available for public download with digital object identifiers
1197 (DOIs). The Earth System Grid Federation (ESGF) is an example of such a system (Petrie et al.,
1198 2021). If applicable, preparing and providing quality-controlled observational datasets for
1199 model evaluation is useful for facilitating analytical efforts (Waliser et al., 2020). Coordinating
1200 the analysis is helpful to avoid duplicative efforts and ensure consistent application of
1201 evaluation metrics. Finally, the design of a coordinated multi-model experiment and all its
1202 procedures should be well documented in publications or permanently archived protocols. It is
1203 advisable to test the multi-model experiment with a small subset of models, before inviting a
1204 large number of participants. Furthermore, it is worth remembering that the science questions
1205 must be appropriate. MIPs require much effort and not every science question needs a MIP to
1206 be answered.

1207 **5 Summary and Key Recommendations**

1208 A range of modeling tools and analysis methods are available for OAE research to address
1209 questions from micro- to global scales; however, each of these tools and methods has limitations
1210 and caveats that model users and users of model-generated outputs need to be aware of.
1211 Furthermore, this new field of research poses questions and challenges that current tools were
1212 not designed to address, necessitating further development.

1213
1214 A common objective of all modeling approaches described in this article is to simulate the
1215 spatio-temporal evolution of carbon chemistry properties in seawater by accounting for the
1216 physical, chemical, and biological processes that determine this evolution. Idealized models,
1217 which neglect some aspects of reality in the interest of simplicity and clarity of assumptions,
1218 have long been used to test basic questions about OAE. As research questions are becoming
1219 more focussed on the practical aspects, feasibility, and ecosystem impacts of OAE, more realistic
1220 models are increasingly desirable. A skillful realistic model can provide spatial and temporal
1221 context for observations, including estimates of properties and fluxes not directly observed.
1222 Such model will include parameterizations of the relevant processes for the research objective to
1223 be addressed and will be constrained by observations that contain sufficient meaningful

1224 information. However, model formulations of several properties and processes relevant to OAE
1225 research remain uncertain or highly simplified. For example, presently used model
1226 representations of alkalinity in seawater are likely inadequate and may require explicit
1227 representation of at least some of the multiple biotic and abiotic sources and sinks of alkalinity;
1228 the mechanisms and triggers for spontaneous calcium carbonate precipitation are only
1229 beginning to be described and not yet represented in models; and the impacts of pH
1230 perturbations on plankton diversity and trophic interactions remain an active area of study and
1231 unaccounted in biogeochemical models. Furthermore, it is difficult to obtain solid constraints on
1232 the seawater carbonate system, especially in sufficient spatial and temporal resolution for
1233 robust model validation and DA. Theoretically, knowledge of two of the carbonate system
1234 parameters allows calculation of the others, but unfortunately $p\text{CO}_2$ and pH, the pair most
1235 accessible to autonomous measurement, results in high uncertainties.

1236 One inherent challenge to OAE research is the multiscale nature of many of the relevant
1237 questions. Different modelling tools are available for different spatial scales. While some
1238 research questions may fall neatly within the limited spatial range of a particular model, many
1239 do not and require a bridging of scales that could be accomplished via new parameterizations
1240 yet to be developed or dynamic coupling of different modeling tools. It is important to
1241 emphasize that models have to be tailored to the questions they are meant to address. This
1242 means considering what level of model complexity is required and seeking parsimonious
1243 representations that are well-supported by empirical constraints.

1244
1245 It is important to note that even after thorough validation, any model simulation will be prone
1246 to errors and uncertainties due to inaccuracies in model inputs, structural uncertainty due to
1247 numerical approximation schemes and insufficient process understanding or representation,
1248 and inaccurate model parameters and parameterizations. Deviations between models and
1249 reality can be reduced by DA, which is typically applied either to systematically optimize
1250 model parameters or to produce optimal estimates of the ocean state. Optimization of model
1251 parameters addresses systematic model errors and biases; it is useful for systematic testing of
1252 different model formulations during model design. State estimation assumes an unbiased
1253 model and addresses unresolved stochasticity, thus leading to model states that are in better
1254 agreement with the observed ocean state. However, successful application of DA critically
1255 requires sufficient observations. Currently, the biggest impediment to implementing data-
1256 assimilative models for OAE research is the sparsity of carbonate system observations. OSSEs,
1257 data-assimilative simulations that inform how to place observing assets most effectively, will
1258 prove useful in this context. It should also be noted that assimilation of carbonate system
1259 parameters is not appropriate when models are applied for MRV.

1260
1261 Uncertainty analysis is a necessary component of any quantitative research and will be an
1262 essential deliverable for effective approaches to MRV. Ensemble-based DA methodologies
1263 provide a useful framework for estimating uncertainty. Consideration of this framework
1264 illustrates the “law of conservation of difficulty” applies here. Quantitative assumptions about
1265 the uncertainty distributions of input data and input parameters, and of structural uncertainties

1266 inherent in the model are required to obtain an uncertainty estimate of the model output, in
1267 other words, difficult assumptions about errors have to be made somewhere. A common
1268 approach to assessing model uncertainty is by coordinated, multi-model intercomparison. Such
1269 studies can be used to explore the range of simulated behaviors and the strengths and
1270 weaknesses of different models and, by elucidating inter-model differences, they can offer
1271 guidance on priority targets for model improvement.

1272

1273 Key recommendations arising from this article are as follows:

1274

1275 • Idealized models of particle-fluid interaction are recommended to address questions
1276 about dissolution and precipitation kinetics at the scale of particles, realistic local-scale
1277 models are recommended for addressing questions about nearfield processes in the
1278 turbulent environment around injection sites, and larger-scale regional or global ocean
1279 models are recommended to support observational design for field experiments, to
1280 demonstrate possible verification frameworks, and to address questions about global-
1281 scale feedbacks on ocean biogeochemistry.

1282 • When simulating OAE approaches that may generate high oversaturation with respect
1283 to carbonate, spontaneous precipitation of carbonates needs to be considered and
1284 appropriate approaches should be developed, e.g., using near-field models to
1285 mechanistically represent this process and a meta-model approach to develop
1286 parameterizations that are suitable for far-field and larger-scale models.

1287 • Shortcomings in current-generation models in terms of representing physiological
1288 responses of the plankton community to OAE (especially when using crushed-rock
1289 feedstocks) need to be recognized, better qualified, and addressed. Empirical research
1290 exploring physiological sensitivities should be used to develop prioritizations of key
1291 model processes comprising early targets for implementation.

1292 • The exchange of solutes between the sediments and overlying water influences the
1293 seawater carbonate system with DIC from the remineralization of organic matter being
1294 returned to overlying water (and alkalinity if this remineralization occurs anaerobically),
1295 dissolution of CaCO_3 releasing alkalinity, and burial of CaCO_3 acting as alkalinity sink.
1296 Accounting for these exchanges between sediments and overlying water and its
1297 variability on tidal, seasonal, interannual, and millennial timescales will likely be
1298 necessary in regional and global biogeochemical models that aim to simulate alkalinity
1299 cycling.

1300 • River inputs of alkalinity and DIC in regional and global ocean biogeochemical models,
1301 including fluxes resulting from land-based CDR applications, should be accurately
1302 accounted for. Efforts should be made to improve quantification of riverine fluxes
1303 resulting from ongoing field trials and commercial applications, and to establish
1304 initiatives to effectively track the solute additions from terrestrial alkalinity
1305 enhancements.

- 1306 • When simulating large-scale deployment of OAE in ocean-only models with prescribed
1307 atmospheric CO₂, the subtle changes in the atmospheric CO₂ inventory resulting from
1308 CDR should be accounted for.
- 1309 • Models should be tailored to the specific questions they are meant to address while
1310 seeking parsimonious representations that are well-supported by empirical constraints.
1311 For example, for the purpose of MRV it may be appropriate to neglect biological
1312 dynamics since the core target is to capture the net air-sea CO₂ exchange associated with
1313 the OAE-induced surface ocean *p*CO₂ anomaly.
- 1314 • Model validation should be an integral part of model implementation and application.
1315 For OAE research, validation is a two-step challenge. First, it is necessary to validate
1316 unperturbed model baselines to gain confidence that the natural variability is
1317 represented appropriately and to quantify model uncertainties. Second, it should be
1318 verified that the model accurately represents the perturbations of an alkalinity addition.
- 1319 • Since no single model validation metric provides a complete picture of a model's skill,
1320 multiple complementary metrics should be used in combination. Furthermore, different
1321 points in space and time, and a breadth of variable types should be part of any
1322 comprehensive validation.
- 1323 • Data assimilation, the process of improving the dynamical behavior of models by
1324 statistically combining them with observations, should be employed in order to obtain
1325 the most accurate model simulations possible, e.g., to optimize model parameters or to
1326 estimate the ocean state. The former addresses systematic errors and biases in models,
1327 while the latter assumes an unbiased model and addresses unresolved stochasticity.
- 1328 • When applying data-assimilative models for quantification of the OAE-induced net CO₂
1329 uptake by calculating the difference between a realistic and a counterfactual simulation,
1330 it is not appropriate to assimilate biogeochemical observations of properties affected by
1331 the alkalinity enhancement as this would eliminate the ability to make valid
1332 comparisons between the two simulation. However, assimilation of observations that
1333 are unaffected by OAE can be applied to both simulations of the pair.
- 1334 • Successful application of DA critically requires sufficient observations either of the
1335 properties that the model parameters to be estimated depend on or of the state variables
1336 that are being estimated. Observing System Simulation Experiments are recommended
1337 to design observing strategies tailored to the needs of specific OAE applications.
- 1338 • Model results should be paired with sound qualitative and quantitative uncertainty
1339 estimates, especially when used for practical decisions. DA methodologies provide a
1340 useful framework for estimating uncertainty, especially ensemble-based methods.
1341 Another common approach to assessing model uncertainty are coordinated, multi-
1342 model studies, commonly called model intercomparison projects or MIPs.

1343

1344 **Acknowledgements**

1345 We thank the Ocean Acidification and other ocean Changes – Impacts and Solutions (OACIS),
1346 an initiative of the Prince Albert II of Monaco Foundation, Judith Meyer, and Angela Stevenson
1347 for their support throughout the project. We extend our gratitude to the Villefranche
1348 Oceanographic Laboratory for supporting the meeting of the lead authors in January 2023.
1349 Jessica Oberlander’s assistance in compiling the bibliography is gratefully acknowledged.

1350

1351 **Competing interests**

1352 KF, AL, and CA are collaborating with Planetary Technology, a climate-tech company, and Pro-
1353 Oceanus Systems Inc., an ocean technology company, as part of an NSERC Alliance Missions
1354 project focussed on OAE; none of the partners have made direct financial contributions to the
1355 project. RM and JO are collaborating with Planetary Technologies, and JO is partially supported
1356 by Planetary Technologies via an NSERC Alliance grant. ML is the Executive Director of
1357 [C]Worthy, LLC, which is a non-profit research organization focused on building tools to
1358 support MRV for ocean CDR. Competing interests are declared in a summary for the entire
1359 volume at: [\url{https://sp.copernicus.org/articles/sp-bpoae-ci-summary.zip}](https://sp.copernicus.org/articles/sp-bpoae-ci-summary.zip).

1360

1361 **Financial support**

1362 The compilation of this article has been supported by the ClimateWorks Foundation (grant no.
1363 22-0296) and the Prince Albert II of Monaco Foundation. KF, AL, RM, and JO acknowledge
1364 funding by NSERC’s Discovery and Alliance Programs. KF, DK, AL, and AO are supported by
1365 the Ocean Alk-Align project funded by Carbon to Sea. RM is supported by the Canada Research
1366 Chairs Program. JPM is supported by the Simons Collaboration on Computational
1367 Biogeochemical Modeling of Marine Ecosystems (grant ID: 459949FY22) and the NOAA Ocean
1368 Acidification Program (grant ID: NA19OAR0170357). DBW is supported by the NASA Earth
1369 science New Investigator Program.

1370 **References**

- 1371
- 1372 Aller, R. C.: Transport and reactions in the bioirrigated zone, in: *The Benthic Boundary Layer*,
1373 edited by: Boudreau, B. P., and Jorgensen, B. B., Oxford University Press, 269-301, ISBN
1374 9780195118810, 2001.
- 1375 Bach, L. T., Gill, S. J., Rickaby, R. E., Gore, S., and Renforth, P.: CO₂ Removal With Enhanced
1376 Weathering and Ocean Alkalinity Enhancement: Potential Risks and Co-benefits for Marine
1377 Pelagic Ecosystems, *Front. Clim.*, 1, <https://doi.org/10.3389/fclim.2019.00007>, 2019.
- 1378 Barrett, P. M., Resing, J. A., Buck, N. J., Freely, R. A., Bullister, J. L., Buck, C. S., and Landing, W.
1379 M.: Calcium carbonate dissolution in the upper 1000 m of the eastern North Atlantic, *Global
1380 Biogeochem. Cy.*, 28, 386-397, <https://doi.org/10.1002/2013GB004619>, 2014.
- 1381 Barton, A. D., Pershing, A. J., Litchman, E., Record, N. R., Edwards, K. F., Kinkel, Z. V., Kiørboe,
1382 T., and Ward, B. A.: The biogeography of marine plankton traits, *Ecol. Lett.*, 16, 522-534,
1383 <https://doi.org/10.1111/ele.12063>, 2013.
- 1384 Bates, N. R., and Merlivat, L.: The influence of short-term wind variability on air-sea CO₂
1385 exchange, *Geophys. Res. Lett.*, 28, 3281-3284, <https://doi.org/10.1029/2001GL012897>, 2001.
- 1386 Bell, T. G., Landwehr, S., Miller, S. D., de Bruyn, W. J., Callaghan, A. H., Scanlon, B., Ward, B.,
1387 Yang, M., and Saltzman, E. S.: Estimation of bubble-mediated air-sea gas exchange from
1388 concurrent DMS and CO₂ transfer velocities at intermediate-high wind speeds, *Atmos. Chem.
1389 Phys.*, 17, 9019-9033, <https://doi.org/10.5194/acp-17-9019-2017>, 2017.
- 1390 Bittig, H. C., Steinhoff, T., Claustre, H., Fiedler, B., Williams, N. L., Sauzède, R., Körtzinger, A.,
1391 and Gattuso, J.-P.: An Alternative to Static Climatologies: Robust Estimation of Open Ocean
1392 CO₂ Variables and Nutrient Concentrations From T, A, and O₂ Data Usin Baysian Neural
1393 Networks, *Front. Mar. Sci.*, 5, 328, <https://doi.org/10/3389/fmars.2018.00328>, 2018.
- 1394 Bleninger, T., and Jirka, G. H.: Near- and far-field model coupling methodology for wastewater
1395 discharges, *Proceedings of the 4th International Symposium in Environmental Hydraulics &
1396 14th Congress of Asia and Pacific Division, International Association of Hydraulic Engineering
1397 and Research*, 15-18, <https://doi.org/10.1201/b16814-73>, 2004.
- 1398 Boudreau, B. P. (Eds.): *Diagenetic Models and their Implementation: Modelling Transport and
1399 Reactions in Aquatic Sciences*, Springer, <https://do.org/10.I007/978-3-642-60421-8>, 1997.
- 1400 Boudreau, B. P., Middelburg, J. J., and Meysman, F. J. R.: Carbonate compensation dynamics,
1401 *Geophys., Res. Lett.*, 37, <https://doi.org/10.1029/2009GL041847>, 2010.
- 1402 Boudreau, B. P., Middelburg, J. J., and Luo, Y.: The role of calcification in carbonate
1403 compensation, *Nat. Geosci.*, 11, 894-900, <https://doi.org/10.1038/s41561-018-0259-5>, 2018.

1404 Boyd, P.W., Claustre, H., Legendre, L., Gattuso, J.-P., and Le Traon, P.-Y.: Operational
1405 monitoring of open-ocean carbon dioxide removal deployments: Detection, attribution, and
1406 determination of side effects, in: *Frontiers in Ocean Observing: Emerging Technologies for*
1407 *Understanding and Managing a Changing Ocean*, edited by: Kappel, E. S., Cullen, V., Costello,
1408 M. J., Galgani, L., Gordó-Vilaseca, C., Govindarajan, A., Kouhi, S.,
1409 Lavin, C., McCartin, L., Müller, J. D., Pirenne, B., Tanhua, T., Zhao, Q., and Zhao, S.,
1410 *Oceanography*, 36(Supplement 1), 2–10, <https://doi.org/10.5670/oceanog.2023.s1.2>, 2023.

1411 Briggs, E. M., Sandoval, S., Erten, A., Takeshita, Y., Kummel, A. C., and Martz, T. R.: Solid state
1412 sensor for simultaneous measurement of total alkalinity and pH of seawater, *ACS Sens.*, 2, 1302-
1413 1309, <https://doi.org/10.1021/acssensors.7b00305>, 2017.

1414 Burdige, D. J.: Preservation of Organic Matter in Marine Sediments: Controls, Mechanisms, and
1415 an Imbalance in Sediment Organic Carbon Budgets?, *Chem. Rev.*, 107, 467-485,
1416 <https://doi.org/10.1021/cr050347q>, 2007.

1417 Burt, D. J., Fröb, F., and Ilyina, T.: The sensitivity of the marine carbonate system to regional
1418 ocean Alkalinity Enhancement. *Front. Clim.*, 3, <https://doi.org/10.3389/fclim.2021.624075>, 2021.

1419 Bushinsky, S.M., Takeshita, Y., and Williams, N. L.: Observing changes in ocean carbonate
1420 chemistry: Our autonomous future, *Current Climate Change Reports* 5, 207–220,
1421 <https://doi.org/10.1007/s40641-019-00129-8>, 2019.

1422 Carrassi, A., Bocquet, M., Bertino, L., and Evensen, G.: Data assimilation in the geosciences: An
1423 overview of methods, issues, and perspectives, *WIREs Clim Change*, 9,
1424 <https://doi.org/10.1002/wcc.535>, 2018.

1425 Carroll, D., Menemenlis, D., Adkins, J. F., Bowman, K. W., Brix, H., Dutkiewicz, S., Fenty, I.,
1426 Gierach, M. M., Hill, C., Jahn, O., Landschützer, P., Lauderdale, J. M., Liu, J., Manizza, M.,
1427 Naviaux, J. D., Rödenbeck, C., Schimel, D. S. Van der Stockem T., and Zhang, H.: The ECCO-
1428 Darwin data-assimilative global ocean biogeochemistry model: Estimates of seasonal to
1429 multidecadal surface ocean $p\text{CO}_2$ and air-sea CO_2 flux, *J. Adv. Model. Earth Sy.*, 12,
1430 e2019MS001888. <https://doi.org/10.1029/2019MS001888>, 2020.

1431 Caserini, S., Pagano, D., Campo, F., Abbà, A., De Marco, S., Righi, D., Renforth, P., and Grosso,
1432 M.: Potential of maritime transport for ocean liming and atmospheric CO_2 removal, *Front.*
1433 *Clim.*, 3, <https://doi.org/10.3389/fclim.2021.575900>, 2021.

1434 Ciavatta, S., Brewin, R. J. W., Skákala, J., Polimene, L., de Mora, L., Artioli, Y., and Allen, J. I.:
1435 Assimilation of ocean-color plankton functional types to improve marine ecosystem
1436 simulations, *J. Geophys. Res. Oceans*, 123, 834–854, <https://doi.org/10.1002/2017JC013490>, 2018.

1437 Chai, F., Johnson, K. S., Claustre, H., Xing, X., Wang, Y., Boss, E., Riser, S., Fennel, K., Schofield,
1438 O., and Sutton, A.: Monitoring ocean biogeochemistry with autonomous platforms, *Nat. Rev.*
1439 *Earth Environ.*, 1, 315–326, <https://doi.org/10.1038/s43017-020-0053-y>, 2020.

1440 Chang, Y. S., and Scotti, A.: Modeling unsteady turbulent flows over ripples: Reynolds-
1441 averaged Navier-Stokes equations (RANS) versus large-eddy simulation (LES), *J. Geophys.*
1442 *Res.-Oceans*, 109, C9, <https://doi.org/10.1029/2003JC002208>, 2004.

1443 Chua, E. J., Huettel, M., Fennel, K., and Fulweiler, R. W.: A case for addressing the unresolved
1444 role of permeable shelf sediments in ocean denitrification, *Limnol. Oceanogr. Letters*, 7, 11-25
1445 <https://doi.org/10.1002/lol2.10218>, 2022.

1446 CMEMS 2023. Global Ocean Physics Analysis and Forecast. E.U. Copernicus Marine Service
1447 Information (CMEMS). Marine Data Store (MDS). DOI: 10.48670/moi-00016 (Accessed on 06-10-
1448 2023)

1449 Cossarini, G., Mariotti, L., Feudale, L., Mignot, A., Salon, S., Taillandier, V., Teruzzi, A., and
1450 D'Ortenzio, F.: Towards operational 3D-Var assimilation of chlorophyll Biogeochemical-Argo
1451 float data into a biogeochemical model of the Mediterranean Sea, *Ocean Modell*, 133, 112–128,
1452 <https://doi.org/10.1016/j.ocemod.2018.11.005>, 2019.

1453 Cullison Gray, S. E., DeGrandpre, M. D., Moore, T. S., Martz, T. R., Friederich, G. E., and
1454 Johnson, K. S.: Applications of *in situ* pH measurements for inorganic carbon calculations, *Mar.*
1455 *Chem.*, 125, 82-90, <https://doi.org/10.1016/j.marchem.2011.02.005>, 2011.

1456 Denvil-Sommer, A., Gehlen, M., and Vrac, M.: Observation system simulation experiments in
1457 the Atlantic Ocean for enhanced surface ocean pCO₂ reconstructions, *Ocean Sci.*, 17, 1011–1030,
1458 <https://doi.org/10.5194/os-17-1011-2021>, 2021.

1459 Dickson, A. G., and Riley, J. P.: The estimation of acid dissociation constants in seawater media
1460 from potentiometric titrations with strong base. I. The ionic product of water - K_w , *Mar. Chem.*,
1461 7, 89-99, [https://doi.org/10.1016/0304-4203\(79\)90001-X](https://doi.org/10.1016/0304-4203(79)90001-X), 1979.

1462 Doney, S. C., Lima, I., Moore, J. K., Lindsay, K., Behrenfeld, M. J., Westberry, T. K., Mahowald,
1463 N., Glover, D. M., and Takahashi, T.: Skill metrics for confronting global upper ocean
1464 ecosystem-biogeochemistry models against field and remote sensing data, *J. Mar. Syst.*, 76, 95-
1465 112, <https://doi.org/10.1016/j.jmarsys.2008.05.015>, 2009.

1466 Dowd, M., Jones, E., and Parslow, J.: A statistical overview and perspectives on data
1467 assimilation for marine biogeochemical models, *Environmetrics*, 25, 203-213,
1468 <https://doi.org/10.1002/env.2264>, 2014.

1469 ECMWF 2023. European Centre for Medium-Range Weather Forecasts (ECMWF) IFS CY41r2
1470 high-resolution operational forecasts (Accessed on 06-10-2023).

1471 Emerson, S. R., and Archer, D.: Calcium carbonate preservation in the ocean, *Philos. T. R. Soc. S-*
1472 *A.*, 331, 29-40, <https://doi.org/10.1098/rsta.1990.0054>, 1990.

1473 Eyring, V., Bony, S., Meehl, G. A., Senior, C. A., Stevens, B., Stouffer, R. J., and Taylor, K. E.:
1474 Overview of the Coupled Model Intercomparison Project Phase 6 (CMIP6) experimental design

1475 and organization, *Geosci. Model Dev.*, 9, 1937–1958, <https://doi.org/10.5194/gmd-9-1937-2016>,
1476 2016.

1477 Fairall, C. W., Hare, J. E., Edson, J. B., and McGillis, W.: Parameterization and
1478 micrometeorological measurement of air-sea gas transfer, *Bound.-Lay. Meteorol.*, 96, 63-106,
1479 <https://doi.org/10.1023/A:1002662826020>, 2000.

1480 Fakhraee, M., Li, Z., Planavsky, N. J., and Reinhard, C. T.: A biogeochemical model of mineral-
1481 based ocean alkalinity enhancement: impacts on the biological pump and ocean carbon uptake,
1482 *Environ. Res. Lett.*, 18, 044047, <https://doi.org/10.1088/1748-9326/acc9d4>, 2023.

1483 Farsoiyya, P. K., Magdelaine, Q., Antkowiak, A., Popinet, S., and Deike, L.: Direct numerical
1484 simulations of bubble-mediated gas transfer and dissolution in quiescent and turbulent flows, *J.*
1485 *Fluid Mech.*, 954, A29, <https://doi.org/10.1017/jfm.2022.994>, 2023.

1486 Fassbender, A. J. Sabine, C. L., Lawrence-Slavas, N., De Carlo, E. H., Meinig, C., and Maenner
1487 Jones, S.: Robust sensor for extended autonomous measurements of surface ocean dissolved
1488 inorganic carbon, *Environ. Sci. Technol.*, 49, 3628-3635, <https://doi.org/10.1021/es5047183>, 2015.

1489 Feng, E. Y., Koeve, W., Keller, D. P., and Oeschles, A.: Model-Based Assessment of the CO₂
1490 Sequestration Potential of Coastal Ocean Alkalinization, *Earth's Future*, 5, 1252-1266,
1491 <https://doi.org/10.1002/2017EF000659>, 2017.

1492 Fennel, K., Losch, M., Schröter, J., and Wenzel, M.: Testing a marine ecosystem model:
1493 sensitivity analysis and parameter optimization, *J. Marine Syst.*, 28, 45-63,
1494 [https://doi.org/10.1016/S0924-7963\(00\)00083-X](https://doi.org/10.1016/S0924-7963(00)00083-X), 2001.

1495 Fennel, K., Wilkin, J., Previdi, M., and Najjar, R.: Denitrification effects on air-sea CO₂ flux in the
1496 coastal ocean: Simulations for the Northwest North Atlantic, *Geophys. Res. Lett.*, 35, L24608,
1497 <https://doi.org/10.1029/2008GL036147>, 2008.

1498 Fennel, K., Gehlen, M., Brasseur, P., Brown, C. W., Ciavatta, S., Cossarini, G., Crise, A.,
1499 Edwards, C. A., Ford, D., Friedrichs, M. A. M., Gregoire, M., Jones, E., Kim, H-C., Lamouroux,
1500 J., Murtugudde, R., Perruche, C., and the GODAE OceanView Marine Ecosystem Analysis and
1501 Prediction Task Team: Advancing Marine Biogeochemical and Ecosystem Reanalyses and
1502 Forecasts as Tools for Monitoring and Managing Ecosystem Health, *Front. Mar. Sci.*, 6, 89,
1503 <https://doi.org/10.3389/fmars.2019.00089>, 2019.

1504 Fennel, K., Mattern, J. P., Doney, S., Bopp, L., Moore, A., Wang, B., and Yu, L.: Ocean
1505 biogeochemical modelling, *Nat. Rev. Methods Primers*, 2, 76, <https://doi.org/10.1038/s43586-022-00154-2>, 2022.

1507 Ferderer, A., Chase, Z., Kennedy, F., Schulz, K. G., and Bach, L. T.: Assessing the influence of
1508 ocean alkalinity enhancement on a coastal phytoplankton community, *Biogeosciences*, 19, 5375–
1509 5399, <https://doi.org/10.5194/bg-19-5375-2022>, 2022.

1510 Foteinis, S., Campbell, J. S., and Renforth, P.: Life cycle assessment of coastal enhanced
1511 weathering for carbon dioxide removal from air, *Environ. Sci. Technol.*, 57, 6169-6178,
1512 <https://doi.org/10.1021/acs.est.2c08633>, 2023.

1513 Ford, D.: Assimilating synthetic Biogeochemical-Argo and ocean colour observations into a
1514 global ocean model to inform observing system design, *Biogeosciences*, 18, 509–534,
1515 <https://doi.org/10.5194/bg-18-509-2021>, 2021.

1516 Fornari, W., Picano, F., Sardinia, G., and Brandt, L.: Reduced particle settling speed in
1517 turbulence, *J. Fluid Mech.*, 808, 153-167, <https://doi.org/10.1017/jfm.2016.648>, 2016.

1518 Fry, C. H., Tyrrell, T., Hain, M. P., Bates, N. R., and Achterberg, E. P.: Analysis of global surface
1519 ocean alkalinity to determine controlling processes, *Mar. Chem.*, 174, 46-57,
1520 <https://doi.org/10.1016/j.marchem.2015.05.003>, 2015.

1521 Fuhr, M., Geilert, S., Schmidt, M., Liebetrau, V., Vogt, C., Ledwig, B., and Wallmann, K.:
1522 Kinetics of olivine weathering in seawater: an experimental study, *Front. Clim.*, 4,
1523 <https://doi.org/10.3389/fclim.2022.831587>, 2022.

1524 Gehlen, M., Bopp, L., and Aumont, O.: Short-term dissolution response of pelagic carbonate
1525 sediments to the invasion of anthropogenic CO₂: A model study, *Geochem. Geophys. Geosy.*, 9,
1526 <https://doi.org/10.1029/2007GC001756>, 2008.

1527 Gent, P. R., and McWilliams, J. C.: Isopycnal Mixing in Ocean Circulation Models, *J. Phys.*
1528 *Oceanogr.*, 20, 150–155, [https://doi.org/10.1175/1520-0485\(1990\)020<0150:IMIOCM>2.0.CO;2](https://doi.org/10.1175/1520-0485(1990)020<0150:IMIOCM>2.0.CO;2),
1529 1990.

1530 Gentile, E., Tarantola, F., Lockley, A., Vivian, C., and Caserini, S.: Use of aircraft in ocean
1531 alkalinity enhancement, *Sci. Total Environ.*, 822, 153484,
1532 <https://doi.org/10.1016/j.scitotenv.2022.153484>, 2022.

1533 Golshan, R., Tejada-Martínez, A. E., Juha, M. J., and Bazilevs, Y.: LES and RANS simulation of
1534 wind-and wave-forced oceanic turbulent boundary layers in shallow water with wall modeling,
1535 *Comput. Fluids*, 145, 96-108, <https://doi.org/10.1016/j.compfluid.2016.05.016>, 2017.

1536 Griffies, S. M., Danabasoglu, G., Durack, P. J., Adcroft, A. J., Balaji, V., Böning, C. W.,
1537 Chassignet, E. P., Curchitser, E., Deshayes, J., Drange, H., Fox-Kemper, B., Gleckler, P. J.,
1538 Gregory, J. M., Haak, H., Hallberg, R. W., Heimbach, P., Hewitt, H. T., Holland, D. M., Ilyina, T.,
1539 Jungclaus, J. H., Komuro, Y., Krasting, J. P., Large, W. G., Marsland, S. J., Masina, S., McDougall,
1540 T. J., Nurser, A. J. G., Orr, J. C., Pirani, A., Qiao, F., Stouffer, R. J., Taylor, K. E., Treguier, A. M.,
1541 Tsujino, H., Uotila, P., Valdivieso, M., Wang, Q., Winton, M., and Yeager, S. G.: OMIP
1542 contribution to CMIP6: experimental and diagnostic protocol for the physical component of the
1543 Ocean Model Intercomparison Project, *Geosci. Model Dev.*, 9, 3231–3296,
1544 <https://doi.org/10.5194/gmd-9-3231-2016>, 2016.

- 1545 Grigoratou, M., Monteiro, F. M., Wilson, J. D., Ridgwell, A., and Schmidt, D. N.: Exploring the
1546 impact of climate change on the global distribution of non-spinose planktonic foraminifera
1547 using a trait-based ecosystem model, *Glob. Change Biol.*, 28, 1063-1076,
1548 <https://doi.org/10.1111/gcb.15964>, 2022.
- 1549 Guo, J. A., Strzepek, R., Willis, A., Ferderer, A., and Bach, L. T.: Investigating the effect of nickel
1550 concentration on phytoplankton growth to assess potential side-effects of ocean alkalinity
1551 enhancement, *Biogeosciences*, 19, 3683–3697, <https://doi.org/10.5194/bg-19-3683-2022>, 2022.
- 1552 Haidvogel, D. B., Arango, H., Budgell, W. P., Cornuelle, B. D., Curchitser, E., Lorenzo, E. D.,
1553 Fennel, K., Geyer, W. R., Hermann, A. J., Lanerolle, L., Levin, J., McWilliams, J. C., Miller, A. J.,
1554 Moore, A. M., Powell, T. M., Shchepetkin, A. F., Sherwood, C. R., Signell, R. P., Warner, J. C.,
1555 and Wilkin, J.: Ocean forecasting in terrain-following coordinates: Formulation and skill
1556 assessment of the Regional Ocean Modeling System, *J. Comput. Phys.*, 227, 3595-3624,
1557 <https://doi.org/10.1016/j.jcp.2007.06.016>, 2008.
- 1558 Hain, M. P., Sigman, D. M., Higgins, J. A., and Haug, G. H.: The effects of secular calcium and
1559 magnesium concentration changes on the thermodynamics of seawater acid/base chemistry:
1560 Implications for Eocene and Cretaceous ocean carbon chemistry and buffering, *Global*
1561 *Biogeochem. Cy.*, 29, 517-533, <https://doi.org/10.1002/2014GB004986>, 2015.
- 1562 Halliwell, G. R., Kourafalou, V., Le Hénaff, M., Shay, L. K., and Atlas, R.: OSSE impact analysis
1563 of airborne ocean surveys for improving upper-ocean dynamical and thermodynamical
1564 forecasts in the Gulf of Mexico, *Prog. Oceanogr.*, 130, 32–46,
1565 <https://doi.org/10.1016/j.pocean.2014.09.004>, 2015.
- 1566 Hartmann, J., Suitner, N., Lim, C., Schneider, J., Marín-Samper, L., Arístegui, J., Renforth, P.,
1567 Taucher, J., and Riebesell, U.: Stability of alkalinity in ocean alkalinity enhancement (OAE)
1568 approaches - consequences for durability of CO₂ storage, *Biogeosciences*, 20, 781-802,
1569 <https://doi.org/10.5194/bg-20-781-2023>, 2023.
- 1570 Harvey, L. D. D.: Mitigating the atmospheric CO₂ increase and ocean acidification by adding
1571 limestone powder to upwelling regions, *J. Geophys. Res.*, 113, C4,
1572 <https://doi.org/10.1029/2007JC004373>, 2008.
- 1573 He, J., and Tyka, M. D.: Limits and CO₂ equilibration of near-coast alkalinity enhancement,
1574 *Biogeosciences*, 20, 27–43, <https://doi.org/10.5194/bg-20-27-2023>, 2023.
- 1575 Heuzé, C.: Antarctic Bottom Water and North Atlantic Deep Water in CMIP6 models, *Ocean*
1576 *Sci.*, 17, 59–90, <https://doi.org/10.5194/os-17-59-2021>, 2021.
- 1577 Hinrichs, C., Köhler, P., Völker, C., and Hauck, J.: Alkalinity biases in CMIP6 Earth System
1578 Models and implications for simulated CO₂ drawdown via artificial alkalinity enhancement,
1579 *Biogeosci. Discuss.*, <https://doi.org/10.5194/bg-2023-26>, 2023.

1580 Ho, D. T., Bopp, L., Palter, J. B., Long, M. C., Boyd, P., Neukermans, G., and Bach, L.:
1581 Monitoring, Reporting, and Verification for Ocean Alkalinity Enhancement, in: Guide to Best
1582 Practices in Ocean Alkalinity Enhancement Research (OAE Guide 23), edited by: Oschlies, A.,
1583 Stevenson, A., Bach, L., Fennel, K., Rickaby, R., Satterfield, T., Webb, R., and Gattuso, J.-P.,
1584 Copernicus Publications, State Planet, <https://doi.org/10.-XXXXX>, 2023.

1585 Hoffman, R. N. and Atlas, R.: Future observing system simulation experiments, *B. Am.*
1586 *Meteorol. Soc.*, 97, 1601–1616, <https://doi.org/10.1175/BAMS-D-15-00200.1>, 2016.

1587 House, K. Z., House, C. H., Schrag, D. P., and Aziz, M. J.: Electrochemical acceleration of
1588 chemical weathering for carbon capture and sequestration, *Enrgy. Proced.*, 1, 4953-4960,
1589 <https://doi.org/10.1016/j.egypro.2009.02.327>, 2009.

1590 Hu, J., Fennel, K., Mattern, J. P., and Wilkin, J.: Data assimilation with a local Ensemble Kalman
1591 Filter applied to a three-dimensional biological model of the Middle Atlantic Bight,
1592 *J. Marine Syst.*, 94, 145-156, <https://doi.org/j.jmarsys.2011.11.016>, 2012.

1593 Huettel, M., Berg, P., and Kostka, J. E.: Benthic exchange and biogeochemical cycling in
1594 permeable sediments, *Ann. Rev. Mar. Sci.*, 6, 23–51, <https://doi.org/10.1146/annurev-marine-051413-012706>, 2014.

1596 Ilyina, T., Wolf-Gladrow, D., Munhoven, G., and Heinze, C.: Assessing the potential of calcium-
1597 based artificial ocean alkalization to mitigate rising atmospheric CO₂ and ocean acidification,
1598 *Geophys. Res. Lett.*, 40, 5909-5914, <https://doi.org/10.1002/2013GL057981>, 2013.

1599 IPCC: Climate Change 2013: The Physical Science Basis, Contribution of Working Group I to the
1600 Fifth Assessment Report of the Intergovernmental Panel on Climate Change, edited by: Stocker,
1601 T. F., Qin, D., Plattner, G.-K., Tignor, M., Allen, S. K., Boschung, J., Nauels, A., Xia, Y., Bex, V.,
1602 Midgley, P. M., Cambridge University Press, 1585 pp., ISBN 978-92-9169-138-8, 2013.

1603 Jahnke, R. A.: Global synthesis, in: Carbon and nutrient fluxes in continental margins: A global
1604 synthesis, edited by: Liu, K.-K., Atkinson, L., Quiñones, R., and Talaue-McManus, L., Springer,
1605 Berlin, Heidelberg, Germany, 597–615, <https://doi.org/10.1007/978-3-540-92735-8>, 2010.

1606 Jirka, G. H., Doneker, R. L., and Hinton, S. W.: User’s manual for CORMIX: A hydrodynamic
1607 mixing zone model and decision support system for pollutant discharges into surface waters, U.
1608 S. Environmental Protection Agency, Washington, D. C., 1996.

1609 Juckes, M., Taylor, K. E., Durack, P. J., Lawrence, B., Mizielinski, M. S., Pamment, A.,
1610 Peterschmitt, J.-Y., Rixen, M., and Sényesi, S.: The CMIP6 Data Request (DREQ, version 01.00.31),
1611 *Geosci. Model Dev.*, 13, 201–224, <https://doi.org/10.5194/gmd-13-201-2020>, 2020.

1612 Keller, D. P., Oschlies, A., and Eby, M.: A new marine ecosystem model for the University of
1613 Victoria Earth System Climate Model, *Geosci. Model Dev.*, 5, 1195–1220,
1614 <https://doi.org/10.5194/gmd-5-1195-2012>, 2012.

1615 Keller, D. P., Feng, E. Y., and Oschlies, A.: Potential climate engineering effectiveness and side
1616 effects during a high carbon dioxide-emission scenario, *Nat. Commun.*, 5, 3304,
1617 <https://doi.org/10.1038/ncomms4304>, 2014.

1618 Keller, D. P., Lenton, A., Scott, V., Vaughan, N. E., Bauer, N., Ji, D., Jones, C. D., Kravitz, B.,
1619 Muri, H., and Zickfeld, K.: The Carbon Dioxide Removal Model Intercomparison Project
1620 (CDRMIP): rationale and experimental protocol for CMIP6, *Geosci. Model Dev.*, 11, 1133–1160,
1621 <https://doi.org/10.5194/gmd-11-1133-2018>, 2018

1622 Kitagawa, G.: A self-organizing state-space model. *J. Am. Stat. Assoc.*, 93, 1203–1215,
1623 <https://doi.org/10.2307/2669862>, 1998.

1624 Ko, Y. H., Lee, K., Eom, K. H., and Han, I.-S.: Organic alkalinity produced by phytoplankton
1625 and its effect on the computation of ocean carbon parameters, *Limnol. Oceanogr.*, 61, 1462-1471,
1626 <https://doi.org/10.1002/lno.10309>, 2016.

1627 Koeve, W., and Oschlies, A.: Potential impact of DOM accumulation on fCO₂ and carbonate ion
1628 computations in ocean acidification experiments, *Biogeosciences*, 9, 3787-3798,
1629 <https://doi.org/10.5194/bg-9-3787-2012>, 2012.

1630 Köhler, P., Hartmann, J., and Wolf-Gladrow, D. A.: Geoengineering potential of artificially
1631 enhanced silicate weathering of olivine, *Proc. Natl. Acad. Sci. U. S. A.*, 107, 20228-20233,
1632 <https://doi.org/10.1073/pnas.1000545107>, 2010.

1633 Köhler, P., Abrams, J. F., Völker, C., Hauck, J., and Wolf-Gladrow, D. A.: Geoengineering
1634 impact of open ocean dissolution of olivine on atmospheric CO₂, surface ocean pH and marine
1635 biology, *Environ. Res. Lett.*, 8, 014009, <https://doi.org/10.1088/1748-9326/8/1/014009>, 2013.

1636 Krumhardt, K. M., Lovenduski, N. S., Iglesias-Rodriguez, M. D., and Lkeypas, J. A.:
1637 Coccolithophore growth and calcification in a changing ocean, *Prog. Oceanogr.*, 159, 276-295,
1638 <https://doi.org/10.1016/j.pocean.2017.10.007>, 2017.

1639 Laurent, A., Fennel, K., Wilson, R., Lehrter, J., and Devereux, R.: Parameterization of
1640 biogeochemical sediment–water fluxes using in situ measurements and a diagenetic model,
1641 *Biogeosciences*, 13, 77-94, <https://doi.org/10.5194/bg-13-77-2016>, 2016.

1642 Laurent, A., Fennel, K., and Kuhn, A.: An observation-based evaluation and ranking of
1643 historical Earth system model simulations in the northwest North Atlantic Ocean,
1644 *Biogeosciences*, 18, 1803–1822, <https://doi.org/10.5194/bg-18-1803-2021>, 2021.

1645 Laurent, A., Wang, B., Pei, A., Ohashi, K., Sheng, J., Garcia Larez, E., Fradette, C., Rakshit, S.,
1646 Atamanchuk, D., Azetsu-Scott, K., Algar, C., Wallace, D., Burt, W., and K. Fennel: A high-
1647 resolution nested model to study the effects of alkalinity additions in a mid-latitude coastal
1648 fjord, Abstract number: 1486172, presented at the Ocean Sciences Meeting 2024, 18-23 February
1649 2024.

1650 Lellouche, J.-M., Greiner, E., Bourdallé-Badie, R., Garric, G., Melet, A., Dréville, M., Bricaud,
1651 C., Hamon, M., Le Galloudec, O., Regnier, C., Candela, T., Testut, C.-E., Gasparin, F., Ruggiero,
1652 G., Benkiran, M., Drillet, Y., and Le Traon, P.-Y.: The Copernicus Global 1/12° Oceanic and Sea
1653 Ice GLORYS12 Reanalysis, *Front. Earth Sci.*, 9, 698876, <https://doi.org/10.3389/feart.2021.698876>,
1654 2021.

1655 Lewis, E. R., and Wallace, D. W. R.: Program developed for CO2 system calculations,
1656 Environmental System Science Data Infrastructure for a Virtual Ecosystem (ESS-DIVE), United
1657 States, <https://doi.org/10.15485/1464255>, 1998.

1658 Li, G., Iskandarani, M., Le Hénaff, M., Winokur, J., Le Maître, O. P., and Knio, O. M.:
1659 Quantifying initial and wind forcing uncertainties in the Gulf of Mexico, *Computat. Geosci.*, 20,
1660 1133-1153, <https://doi.org/10.1007/s10596-016-9581-4>, 2016.

1661 Liang, J.-H., McWilliams, J. C., Sullivan, P. P., and Baschek, B.: Modeling bubbles and dissolved
1662 gases in the ocean, *J. Geophys. Res.-Oceans*, 116, C3, <https://doi.org/10.1029/2010JC006579>, 2011.

1663 Liang, J.-H., Deutsch, C., McWilliams, J. C., Baschek, B., Sullivan, P. P., and Chiba, D.:
1664 Parameterizing bubble-mediated air-sea gas exchange and its effect on ocean ventilation, *Global
1665 Biogeochem. Cy.*, 27, 894-905, <https://doi.org/10.1002/gbc.20080>, 2013.

1666 Lohrenz, S. E., Cai, W.-J., Chakraborty, S., Huang, W.-J., Guo, X., He, R., Xue, Z., Fennel, K.,
1667 Howden, S., and Tian, H.: Satellite estimation of coastal pCO₂ and air-sea flux of carbon dioxide
1668 in the northern Gulf of Mexico, *Remote Sens. Environ.*, 207, 71-83,
1669 <https://doi.org/10.1016/j.rse.2017.12.039>, 2018.

1670 Long, J. S., Hu, C., Robbins, L. L., Byrne, R. H., Paul, J. H., and Wolny, J. L.: Optical and
1671 biochemical properties of a southwest Florida whiting event, *Estuar. Coast. Shelf S.*, 196, 258-
1672 268, <https://doi.org/10.1016/j.ecss.2017.07.017>, 2017.

1673 Long, M. C., Moore, J. K., Lindsay, K., Levy, M., Doney, S. C., Luo, J. Y., Krumhardt, K. M.,
1674 Letscher, R. T., Grover, M., and Sylvester, Z. T.: Simulations with the marine biogeochemistry
1675 library (MARBL), *J. Adv. Model. Earth Syst.*, <https://doi.org/10.1029/2021ms002647>, 2021.

1676 Mattern, J.P., Fennel, K., and Dowd, M.: Estimating time-dependent parameters for a biological
1677 ocean model using an emulator approach, *J. Mar. Syst.*, 96–97, 32-47,
1678 <https://doi.org/10.1016/j.jmarsys.2012.01.015>, 2012.

1679 Mattern, J. P., Fennel, K., and Dowd, M.: Periodic time-dependent parameters improving
1680 forecasting abilities of biological ocean models, *Geophys. Res. Lett.*, 41, 6848-6854,
1681 <https://doi.org/10.1002/2014GL061178>, 2014.

1682 Mattern, J. P., Song, H., Edwards, C. A., Moore, A. M., and Fiechter, J.: Data assimilation of
1683 physical and chlorophyll observations in the California Current System using two
1684 biogeochemical models, *Ocean Model.*, 109, 55–71, <https://doi.org/10.1016/j.ocemod.2016.12.002>,
1685 2017.

1686 Maurer, T. L., Plant, J. N., and Johnson, K. S.: Delayed-Mode Quality Control of Oxygen,
1687 Nitrate, and pH Data on SOCCOM Biogeochemical Profiling Floats, *Front. Mar. Sci.*, 8,
1688 <https://doi.org/10.3389/fmars.2021.683207>, 2021.

1689 McLaughlin, K., Weisberg, S. B., Dickson, A. G., Hofmann, G., Newton, J. A., Aseltine-Neilson,
1690 D., Barton, A., Cudd, S., Feely, R. A., Jefferds, I. W., Jewett, E. B., King, T., Langdon, C. J.,
1691 McAfee, S., Pleschner-Steele, D., and Steele, B.: Core principles of the California current
1692 acidification network: Linking chemistry, physics, and ecological effects, *Oceanography*, 28,
1693 160-169, <http://www.jstor.org/stable/24861878>, 2015.

1694 Mengis, N., Keller, D. P., MacDougall, A. H., Eby, M., Wright, N., Meissner, K. J., Oschlies, A.,
1695 Schmittner, A., MacIsaac, A. J., Matthews, H. D., and Zickfeld, K.: Evaluation of the University
1696 of Victoria Earth System Climate Model version 2.10 (UVic ESCM 2.10), *Geosci. Model Dev.*, 13,
1697 4183–4204, <https://doi.org/10.5194/gmd-13-4183-2020>, 2020.

1698 Mensa, J. A., Özgökmen, T. M., Poje, A. C., and Imberger, J.: Material transport in a convective
1699 surface mixed layer under weak wind forcing, *Ocean Model.*, 96, 226-242,
1700 <https://doi.org/10.1016/j.ocemod.2015.10.006>, 2015.

1701 Meysman, F. J. R., Middelburg, J. J., and Heip, C. H. R.: Bioturbation: a fresh look at Darwin's
1702 last idea, *Trends Ecol. Evol.*, 21, 688-695, <https://doi.org/10.1016/j.tree.2006.08.002>, 2006.

1703 Meysman, F. J. R., and Montserrat, F.: Negative CO₂ emissions via enhanced silicate weathering
1704 in coastal environments, *Biol. Lett.*, 13, 20160905, <http://doi.org/10.1098/rsbl.2016.0905>, 2017.

1705 Middelburg, J. J., Soetaert, K., and Hagens, M.: Ocean Alkalinity, Buffering and Biogeochemical
1706 Processes, *Rev. Geophys.*, 58, e2019RG000681, <https://doi.org/10.1029/2019RG000681>, 2020.

1707 Millero, F. J.: The Marine Inorganic Carbon Cycle, *Chem. Rev.*, 107, 308-341,
1708 <https://doi.org/10.1021/cr0503557>, 2007.

1709 Mongin, M., Baird, M. E., Tilbrook, B., Matear, R. J., Lenton, A., Herzfeld, M., Wild-Allen, K.,
1710 Skerratt, J., Margvelashvili, N., Robson, B. J., Duarte, C. M., Gustafsson, M. S. M., Ralph, P. J.,
1711 and Steven, A. D. L.: The exposure of the Great Barrier Reef to ocean acidification, *Nat.*
1712 *Commun.*, 7, 10732, <https://doi.org/10.1038/ncomms10732>, 2016.

1713 Mongin, M., Baird, M. E., Lenton, A., Neill, C., and Akl, J.: Reversing ocean acidification along
1714 the Great Barrier Reef using alkalinity injection, *Environ. Res. Lett.*, 16, 064068,
1715 <https://doi.org/10.1088/1748-9326/ac002d>, 2021.

1716 Montserrat, F., Renforth, P., Hartmann, J., Leermakers, M., Knops, P., and Meysman, F. J. R.:
1717 Olivine dissolution in seawater: Implications for CO₂ sequestration through enhanced
1718 weathering in coastal environments, *Environ. Sci. Technol.*, 51, 3960-3972,
1719 <https://doi.org/10.1021/acs.est.6b05942>, 2017.

1720 Moras, C. A., Bach, L. T., Cyronak, T., Joannes-Boyau, R., and Schulz, K. G.: Ocean alkalinity
1721 enhancement – avoiding runaway CaCO₃ precipitation during quick and hydrated lime
1722 dissolution, *Biogeosciences*, 19, 3537–3557, <https://doi.org/10.5194/bg-19-3537-2022>, 2022.

1723 Moriarty, J. M., Harris, C. K., Fennel, K., Friedrichs, M. A. M., Xu, K., and Rabouille, C.: The
1724 roles of resuspension, diffusion and biogeochemical processes on oxygen dynamics offshore of
1725 the Rhône River, France: a numerical modeling study, *Biogeosciences*, 14, 1919-1946,
1726 <https://doi.org/10.5194/bg-14-1919-2017>, 2017.

1727 Moriarty, J.M., Harris, C. K., Friedrichs, M. A. M., Fennel, K., and Xu, K.: Impact of seabed
1728 resuspension on oxygen and nitrogen dynamics in the northern Gulf of Mexico: A numerical
1729 modeling study, *J. Geophys. Res-Oceans*, 123, 7237-7263, <https://doi.org/10.1029/2018JC013950>,
1730 2018.

1731 Morse, J. W., Mucci, A., and Millero, F. J.: The solubility of calcite and aragonite in seawater of
1732 35‰ salinity at 25°C and atmospheric pressure, *Geochim. Cosmochim. Ac.*, 44, 85-94,
1733 [https://doi.org/10.1016/0016-7037\(80\)90178-7](https://doi.org/10.1016/0016-7037(80)90178-7), 1980.

1734 Mu, L., Palter, J. B., and Wang, H.: Considerations for hypothetical carbon dioxide removal via
1735 alkalinity addition in the Amazon River watershed, *EGUsphere* [preprint],
1736 <https://doi.org/10.5194/egusphere-2022-1505>, 2023.

1737 Naveira Garabato, A. C., MacGilchrist, G. A., Brown, P. J., Evans, D. G., Meijers, A. J. S., and
1738 Zika, J. D.: High-latitude ocean ventilation and its role in Earth’s climate transitions, *Philos.*
1739 *Trans. A Math. Phys. Eng. Sci.*, 375, <https://doi.org/10.1098/rsta.2016.0324>, 2017.

1740 Negrete-García, G., Luo, J. Y., Long, M. C., Lindsay, K., Levy, M., and Barton, A. D.: Plankton
1741 energy flows using a global size-structured and trait-based model, *Prog. Oceanogr.*, 209, 102898,
1742 <https://doi.org/10.1016/j.pocean.2022.102898>, 2022.

1743 Oschlies, A.: Impact of atmospheric and terrestrial CO₂ feedbacks on fertilization-induced
1744 marine carbon uptake, *Biogeosciences*, 6, 1603–1613, <https://doi.org/10.5194/bg-6-1603-2009>,
1745 2009.

1746 Paquay, F. S., and Zeebe, R. E.: Assessing possible consequences of ocean liming on ocean pH,
1747 atmospheric CO₂ concentration and associated costs, *Int. J. Green. Gas Con.*, 17, 183-188,
1748 <https://doi.org/10.1016/j.ijggc.2013.05.005>, 2013.

1749 Pascoe, C., Lawrence, B. N., Guilyardi, E., Jukes, M., and Taylor, K. E.: Documenting numerical
1750 experiments in support of the Coupled Model Intercomparison Project Phase 6 (CMIP6), *Geosci.*
1751 *Model Dev.*, 13, 2149–2167, <https://doi.org/10.5194/gmd-13-2149-2020>, 2020.

1752 Paul, A. J., and Bach, L. T.: Universal response pattern of phytoplankton growth rates to
1753 increase CO₂, *New Phytol.*, 228, 1710-1716, <https://doi.org/10.1111/nph.16806>, 2020.

- 1754 Paulmier, A., Kriest, I., and Oschlies, A.: Stoichiometries of remineralisation and denitrification
1755 in global biogeochemical ocean models, *Biogeosciences*, 6, 923–935, [https://doi.org/10.5194/bg-6-](https://doi.org/10.5194/bg-6-923-2009)
1756 923-2009, 2009.
- 1757 Petrie, R., Denvil, S., Ames, S., Levavasseur, G., Fiore, S., Allen, C., Antonio, F., Berger, K.,
1758 Bretonnière, P.-A., Cinquini, L., Dart, E., Dwarakanath, P., Druken, K., Evans, B., Franchistéguy,
1759 L., Gardoll, S., Gerbier, E., Greenslade, M., Hassell, D., Iwi, A., Juckes, M., Kindermann, S.,
1760 Lacinski, L., Mirto, M., Nasser, A. B., Nassisi, P., Nienhouse, E., Nikonov, S., Nuzzo, A.,
1761 Richards, C., Ridzwan, S., Rixen, M., Serradell, K., Snow, K., Stephens, A., Stockhause, M.,
1762 Vahlenkamp, H., and Wagner, R.: Coordinating an operational data distribution network for
1763 CMIP6 data, *Geosci. Model Dev.*, 14, 629–644, <https://doi.org/10.5194/gmd-14-629-2021>, 2021.
- 1764 Raimondi, L., Matthews, J. B. R., Atamanchuk, D., Azetsu-Scott, K., and Wallace, D. W. R.: The
1765 internal consistency of the marine carbon dioxide system for high latitude shipboard and *in situ*
1766 monitoring, *Mar. Chem.*, 213, 49-70, <https://doi.org/10.1016/j.marchem.2019.03.001>, 2019.
- 1767 Ramadhan, A., Wagner, G., Hill, C., Campin, J.-M., Churavy, V., Besard, T., Souza, A., Edelman,
1768 A., Ferrari, R., and Marshall, J.: Oceananigans.jl: Fast and friendly geophysical fluid dynamics in
1769 GPUs, *J. Open Source Softw.*, 5, <https://doi.org/10.21105/joss.02018>, 2020.
- 1770 Rau, G. H., McLeod, E. L., and Hoegh-Guldberg, O.: The need for new ocean conservation
1771 strategies in a high-carbon dioxide world, *Nat. Clim. Change*, 2, 720-724,
1772 <https://doi.org/10.1038/nclimate1555>, 2012.
- 1773 Renforth, P., and Henderson, G.: Assessing ocean alkalinity for carbon sequestration, *Rev.*
1774 *Geophys.*, 55, 636–674, <https://doi.org/10.1002/2016RG000533>, 2017.
- 1775 Riebesell, U., Wold-Gladrow, D. A., and Smetacek, V.: Carbon dioxide limitation of marine
1776 phytoplankton growth rates, *Nature*, 361, 249-251, <https://doi.org/10.1038/361249a0>, 1993.
- 1777 Ringham, M.: High resolution, in-situ studies of seawater carbonate chemistry and carbon
1778 cycling in costal systems using CHANnelized Opticals System II, Ph. D. thesis, Massachusetts
1779 Institute of Technology, 127 pp., <https://hdl.handle.net/1721.1/144860>, 2022.
- 1780 Rothstein, L. M., Cullen, J. J., Abbott, M., Chassignet, E. P., Denman, K., Doney, S. C., Ducklow,
1781 H., Fennel, K., Follows, M., Haidvogel, D., Hofmann, E., Karl, D. M., Kindle, J., Lima, I.,
1782 Maltrud, M., McClain, C., McGillicuddy, D., Olascoaga, M. J., Spitz, Y., Wiggert, J., and Woder,
1783 J.: Modeling Ocean Ecosystems: The PARADIGM Program, *Oceanography*, 19, 22-51,
1784 <https://doi.org/10.5670/oceanog.2006.89>, 2015.
- 1785 Rutherford, K., Fennel, K., Atamanchuk, D., Wallace, D., and Thomas, H.: A modelling study of
1786 temporal and spatial pCO₂ variability on the biologically active and temperature-dominated
1787 Scotian Shelf, *Biogeosciences*, 18, 6271-6286, <https://doi.org/10.5194/bg-18-6271-2021>, 2021.
- 1788 Sarmiento, J. L., and Gruber, N.: *Ocean Biogeochemical Dynamics*, Princeton University Press,
1789 <https://doi.org/10.2307/j.ctt3fgxqx>, 2006.

1790 Sauerland, V., Kriest, I., Oschlies, A., and Srivastav, A.: Multiobjective calibration of a global
1791 biogeochemical ocean model against nutrients, oxygen, and oxygen minimum zones, *J. Adv.*
1792 *Model. Earth Sy.*, 11, 1285–1308, <https://doi.org/10.1029/2018MS001510>, 2019.

1793 Schartau, M., Wallhead, P., Hemmings, J., Löptien, U., Kriest, I., Krishna, S., Ward, B. A.,
1794 Slawig, T., and Oschlies, A.: Reviews and syntheses: parameter identification in marine
1795 planktonic ecosystem modelling, *Biogeosciences*, 14, 1647–1701, [https://doi.org/10.5194/bg-14-](https://doi.org/10.5194/bg-14-1647-2017)
1796 1647-2017, 2017.

1797 Schmittner, A., Oschlies, A., Matthews, H. D., and Galbraith, E. D.: Future changes in climate,
1798 ocean circulation, ecosystems, and biogeochemical cycling simulated for a business-as-usual
1799 CO₂ emission scenario until 4000 AD, *Global Biogeochem. Cy.*, 22,
1800 <https://doi.org/10.1029/2007GB002953>, 2008.

1801 Schulz, K. G., Bach, L. T., and Dickson, A. G.: Seawater carbonate system considerations for
1802 ocean alkalinity enhancement research, in: *Guide to Best Practices in Ocean Alkalinity*
1803 *Enhancement Research (OAE Guide 23)*, edited by: Oschlies, A., Stevenson, A., Bach, L., Fennel,
1804 K., Rickaby, R., Satterfield, T., Webb, R., and Gattuso, J.-P., Copernicus Publications, State
1805 Planet, <https://doi.org/10.-XXXXX>, 2023.

1806 Seitzinger, S. P., Harrison, J. A., Böhlke, J. K., Bouwman, A. F., Lowrance, R., Tobias, C., and
1807 Van Drecht, G.: Denitrification across landscapes and waterscapes: A synthesis, *Ecol. Appl.*, 16,
1808 2064–2090, [https://doi.org/10.1890/1051-0761\(2006\)016\[2064:DALAWA\]2.0.CO;2](https://doi.org/10.1890/1051-0761(2006)016[2064:DALAWA]2.0.CO;2), 2006.

1809 Seitzinger, S. P., Mayorga, E., Bouwman, A. F., Kroeze, C., Beusen, H. W., Billen, G., Van Dracht,
1810 G., Dumont, E., Fekete, B. M., Garnier, J., and Harrison, J. A.: Global river nutrient export: A
1811 scenario analysis of past and future trends, *Global Biogeochem. Cycles*, 24, GB0A08,
1812 <https://doi.org/10.1029/2009GB003587>, 2010.

1813 Shangguan, Q., Prody, A., Wirth, T. S., Briggs, E. M., Martz, T. R., and DeGrandpre, M. D.: An
1814 inter-comparison of autonomous *in situ* instruments for ocean CO₂ measurements under
1815 laboratory-controlled conditions, *Mar. Chem.*, 240, 104085,
1816 <https://doi.org/10.1016/j.marchem.2022.104085>, 2022.

1817 Shchepetkin, A. F., and McWilliams, J. C.: The regional oceanic modeling system (ROMS): a
1818 split-explicit, free-surface, topography-following-coordinate oceanic model, *Ocean Model.*, 9,
1819 347-404, <https://doi.org/10.1016/j.ocemod.2004.08.002>, 2005.

1820 Smagorinsky, J.: General circulation experiments with the primitive equations, *Mon. Weather*
1821 *Rev.*, 91, 99-164, [https://doi.org/10.1175/1520-0493\(1963\)091<0099:GCEWTP>2.3.CO;2](https://doi.org/10.1175/1520-0493(1963)091<0099:GCEWTP>2.3.CO;2), 1963.

1822 Smith, K. M., Hamlington, P. E., Niemeyer, K. E., Fox-Kemper, B., and Lovenduski, N. S.: Effects
1823 of Langmuir turbulence on upper ocean carbonate chemistry, *J. Adv. Model. Earth Sy.*, 10, 3030-
1824 3048, <https://doi.org/10.1029/2018MS001486>, 2018.

1825 Soetaert, K., Hofmann, A. F., Middelburg, J. J., Meysman, F. J. R., and Greenwood, J.: The effect
1826 of biogeochemical processes on pH, *Mar. Chem.*, 105, 30-51,
1827 <https://doi.org/10.1016/j.marchem.2006.12.012>, 2007.

1828 Sonnichsen, C., Atamanchuk, D., Hendricks, A., Morgan, S., Smith, J., Grundke, I., Luy, E., and
1829 Sieben, V. J.: An Automated Microfluidic Analyzer for in-situ Monitoring of Total Alkalinity,
1830 *ACS Sens.*, 8, 344-352, <https://doi.org/10.1021/acssensors.2c02343>, 2023.

1831 Stammer, D.: Global Characteristics of Ocean Variability Estimated from Regional
1832 TOPEX/POSEIDON Altimeter Measurements, *J. Phys. Oceanogr.*, 27, 1743–1769,
1833 [https://doi.org/10.1175/1520-0485\(1997\)027<1743:GCOOVE>2.0.CO;2](https://doi.org/10.1175/1520-0485(1997)027<1743:GCOOVE>2.0.CO;2), 1997.

1834 Stow, C. A., Jolliff, J., McGillicuddy Jr., D. J., Doney, S. C., Allen, J. I., Friedrichs, M. A. M., Rose,
1835 K. A., and Wallhead, P.: Skill assessment for coupled biological/physical models of marine
1836 systems, *J. Mar. Syst.*, 76, 4-15, <https://doi.org/10.1016/j.jmarsys.2008.03.011>, 2009.

1837 Subhas, A. V., Lehmann, N., and Rickaby, R.: Natural Analogs to Ocean Alkalinity
1838 Enhancement, in: *Guide to Best Practices in Ocean Alkalinity Enhancement Research (OAE*
1839 *Guide 23)*, edited by: Oschlies, A., Stevenson, A., Bach, L., Fennel, K., Rickaby, R., Satterfield, T.,
1840 Webb, R., and Gattuso, J.-P., Copernicus Publications, State Planet, <https://doi.org/10.-XXXXX>,
1841 2023.

1842 Subhas, A. V., Dong, S., Naviaux, J. D., Rollins, N. E., Ziveri, P., Gray, W., Rae, J. W. B., Liu, X.,
1843 Bryne, R. H., Chen, S., Moore, C., Martell-Bonnet, L., Steiner, Z., Antler, G., Hu, H., Lunstrum,
1844 A., Hou, Y., Kemnits, N., Stutsman, J., Pallacks, S., Dugenne, M., Quay, P. D., Berelson, W. M.,
1845 and Adkins, J. F.: Shallow calcium carbonate cycling in the North Pacific Ocean, *Global*
1846 *Biogeochem. Cy.*, 36, e2022GB007388, <https://doi.org/10.1029/2022GB007388>, 2022.

1847 Sulpis, O., Jeansseon, E., Dinauer, A., Lauvset, S. K., and Middelburg, J. J.: Calcium carbonate
1848 dissolution patterns in the ocean, *Nat. Geosci.*, 14, 423-428, [https://doi.org/10.1038/s41561-021-](https://doi.org/10.1038/s41561-021-00743-y)
1849 [00743-y](https://doi.org/10.1038/s41561-021-00743-y), 2021.

1850 Takeshita, Y., Jones, B. D., Johnson, K. S., Chavez, F. P., Rudnick, D. L., Blum, M., Conner, K.,
1851 Jensen, S., Long, J. S., Maughan, T., Mertz, K. L., Sherman, J. T., and Warren, J. K.: Accurate pH
1852 and O₂ Measurements from Spray Underwater Gliders, *J. Atmos. Oceanic Technol.*, 38, 181–195,
1853 <https://doi.org/10.1175/JTECH-D-20-0095.1>, 2021.

1854 Taylor, L. L., Quirk, J., Thorley, R. M. S., Kharecha, P. A., Hansen, J., Ridgwell, A., Lomas, M. R.,
1855 Banwart, S. A., and Beerling, D. J.: Enhanced weathering strategies for stabilizing climate and
1856 averting ocean acidification, *Nat. Clim. Change*, 6, 402-406,
1857 <https://doi.org/10.1038/nclimate2882>, 2016.

1858 Taylor, J. R., Smith, K. M., and Vreugdenhil, C. A.: The influence of submesoscales and vertical
1859 mixing on the export of sinking tracers in Large-Eddy Simulations, *J. Phys. Oceanogr.*, 50, 1319-
1860 1339, <https://doi.org/10.1175/JPO-D-19-0267.1>, 2020.

1861 Teruzzi, A., Bolzon, G., Salon, S., Lazzari, P., Solidoro, C., and Cossarini, G.: Assimilation of
1862 coastal and open sea biogeochemical data to improve phytoplankton simulation in the
1863 Mediterranean Sea, *Ocean Modell*, 132, 46–60, <https://doi.org/10.1016/j.ocemod.2018.09.007>,
1864 2018.

1865 Thacker, W. C.: The role of the Hessian matrix in fitting models to measurements, *J. Geophys.*
1866 *Res.-Oceans*, 95, 6177-6196, <https://doi.org/10.1029/JC094iC05p06177>, 1989.

1867 Thacker, W. C., Srinivasan, A., Iskandarani, M., Knio, O. M., and Le Hénaff, M.: Propagating
1868 boundary uncertainties using polynomial expansions, *Ocean Model.*, 43-44, 52-63,
1869 <https://doi.org/10.1016/j.ocemod.2011.11.011>, 2012.

1870 Turner, K. E., Smith, D. M., Katavouta, A., and Williams, R. G.: Reconstructing ocean carbon
1871 storage with CMIP6 Earth system models and synthetic Argo observations, *Biogeosciences*, 20,
1872 1671-1690, <https://doi.org/10.5194/bg-20-1671-2023>, 2023.

1873 Verdy, A., and Mazloff, M. R.: A data assimilating model for estimating Southern Ocean
1874 biogeochemistry, *J. Geophys. Res.*, 122, 6968–6988, <https://doi.org/10.1002/2016JC012650>, 2017.

1875 Waliser, D., Gleckler, P. J., Ferraro, R., Taylor, K. E., Ames, S., Biard, J., Bosilovich, M. G.,
1876 Brown, O., Chepfer, H., Cinquini, L., Durack, P. J., Eyring, V., Mathieu, P.-P., Lee, T., Pinnock,
1877 S., Potter, G. L., Rixen, M., Saunders, R., Schulz, J., Thépaut, J.-N., and Tuma, M.: Observations
1878 for Model Intercomparison Project (Obs4MIPs): status for CMIP6, *Geosci. Model Dev.*, 13, 2945–
1879 2958, <https://doi.org/10.5194/gmd-13-2945-2020>, 2020.

1880 Wang, B., Fennel, K., Yu, L., and Gordon, C.: Assessing the value of biogeochemical Argo
1881 profiles versus ocean color observations for biogeochemical model optimization in the Gulf of
1882 Mexico, *Biogeosciences*, 17, 4059–4074, <https://doi.org/10.5194/bg-17-4059-2020>, 2020.

1883 Wang, B., Laurent, A., and K. Fennel: Numerical dye tracer experiments in Bedford Basin in
1884 support of Ocean Alkalinity Enhancement research, Abstract number: 1479880, presented at the
1885 Ocean Sciences Meeting 2024, 18-23 February 2024.

1886 Wang, H., Pilcher, D. J., Kearney, K. A., Cross, J. N., Shugart, O. M., Eisaman, M. D., and Carter,
1887 B. R.: Simulated impact of ocean alkalinity enhancement on atmospheric CO₂ removal in the
1888 Bering Sea, *Earths Future*, 11, <https://doi.org/10.1029/2022ef002816>, 2023.

1889 Wang, Z. A., Sonnichsen, F. N., Bradley, A. M., Hoering, K. A., Lanagan, T. M., Chu, S. N.,
1890 Hammar, T. R., and Camilli, R.: In situ sensor technology for simultaneous spectrophotometric
1891 measurements of seawater total dissolved inorganic carbon and pH, *Environ. Sci. Technol.*, 49,
1892 4441-4449, <https://doi.org/10.1021/es504893n>, 2015.

1893 Wanninkhof, R.: Relationship between wind speed and gas exchange over the ocean, *J.*
1894 *Geophys. Res.-Oceans*, 97, C5, <https://doi.org/10.1029/92JC00188>, 1992.

1895 Wanninkhof, R.: Relationship between wind speed and gas exchange over the ocean revisited,
1896 *Limnol. Oceanogr. - Meth.*, 12, 351-362, <https://doi.org/10.4319/lom.2014.12.351>, 2014.

- 1897 Whitt, D. B., Lévy, M., and Taylor, J. R.: Submesoscales enhance storm-driven vertical mixing of
1898 nutrients: insights from a biogeochemical large eddy simulation, *J. Geophys. Res.-Oceans*, 124,
1899 8140-8165, <https://doi.org/10.1029/2019JC015370>, 2019.
- 1900 Wilcox, L. J., Allen, R. J., Samset, B. H., Bollasina, M. A., Griffiths, P. T., Keeble, J. M., Lund, M.
1901 T., Makkonen, R., Merikanto, J., O'Donnell, D., Paynter, D. J., Persad, G. G., Rumbold, S. T.,
1902 Takemura, T., Tsigaridis, K., Undorf, S., and Westervelt, D. M.: The Regional Aerosol Model
1903 Intercomparison Project (RAMIP), *Geosci. Model Dev. Discuss.* [preprint],
1904 <https://doi.org/10.5194/gmd-2022-249>, in review, 2022.
- 1905 Wolf-Gladrow, D. A., Zeebe, R. E., Klaas, C., Körtzinger, A., and Dickson, A. G.: Total alkalinity:
1906 The explicit conservative expression and its application to biogeochemical processes, *Mar.*
1907 *Chem.*, 106, 287-300, <https://doi.org/10.1016/j.marchem.2007.01.006>, 2007.
- 1908 Yu, L., Fennel, K., Bertino, L., Gharamti, M. E., and Thompson, K. R.: Insights on multivariate
1909 updates of physical and biogeochemical ocean variables using an Ensemble Kalman Filter and
1910 an idealized model of upwelling, *Ocean Model.*, 126, 13–28,
1911 <https://doi.org/10.1016/j.ocemod.2018.04.005>, 2018.
- 1912 Zeebe, R. E., and Wolf-Gladrow, D. A.: *CO₂ in seawater: equilibrium, kinetics, isotopes*, Gulf
1913 Professional Publishing, 346 pp., ISBN 9780444509468, 2001.
1914